HHS Public Access

Author manuscript

Neuroendocrinology. Author manuscript; available in PMC 2024 March 08.

Published in final edited form as:

Neuroendocrinology. 2023 ; 113(12): 1262–1282. doi:10.1159/000526959.

Impacts of Gestational FireMaster 550 (FM 550) Exposure on the Neonatal Cortex are Sex Specific and Largely Attributable to the Organophosphate Esters

Shannah K Witchey[1], **Michael G. Doyle**[2], **Jacob D. Fredenburg**[1], **Genevieve St. Armour**[1], **Brian Horman**[1], **Melanie T. Odenkirk**[2], **David L. Aylor**[1,3], **Erin S. Baker**[2], **Heather B Patisaul**[3]

[1]Department of Biological Sciences, NC State University

[2]Department of Chemistry, NC State University

[3]Center for Human Health and the Environment, NC State University

Abstract

Introduction: Flame retardants (FRs) are common bodily and environmental pollutants, creating concern about their potential toxicity. We and others have found that the commercial mixture, FireMaster® 550 (FM 550) or its individual brominated (BFR) and organophosphate ester (OPFR) components are potential developmental neurotoxicants. Using Wistar rats, we previously reported developmental exposure to FM 550 or its component classes produced sex- and compound-specific effects on adult socioemotional behaviors. The underlying mechanisms driving the behavioral phenotypes are unknown.

Methods: To further mechanistic understanding, here we conducted transcriptomics in parallel with a novel lipidomics approach using cortical tissues from newborn siblings of the rats in the published behavioral study. Inclusion of lipid composition is significant because it is rarely

Corresponding Author: Heather B. Patisaul PhD, 127 David Clark Labs, NC State University, Box 7619, Raleigh, NC 27695 USA, (919) 515-2501.

Author Contributions:

Shannah K Witchey led the design and execution of the studies, data collection, data analysis, supervision of assisting personnel, manuscript preparation including all figures, tables and supplemental materials, and gave final approval of the version to be published.

Michael G. Doyle performed data analysis for the lipidomics portion of the project and contributed to manuscript preparation and final approval of the version to be published.

Jacob D. Fredenburg performed the transcriptomics analysis in collaboration with Shannah K. Witchey and helped prepare the related figures and tables.

Genevieve St. Armour assisted with animal dosing and care, necropsy, brain microdissection and the nanostring-related work including the preparation of the related methods and results sections.

Brian Horman organized and oversaw all of the animal dosing, housing, and necropsy as well as IACUC protocols, and also assisted with manuscript editing including approval of the final version.

Melanie T. Odenkirk extracted the lipids, aided in analyzing the lipidomics portion of the project and assisted with the manuscript including final version approval.

David L. Aylor led, supervised, and partially funded the transcriptomics work including data analysis and interpretation, drafting of the transcriptomics portion of the manuscript, and revising it for intellectual content.

Erin S. Baker, led, supervised, and partially funded the lipidomics work including the development of appropriate methods, drafting of the lipidomics portion of the manuscript, and revising it for intellectual content.

Heather B Patisaul conceived of the project, funded the majority of the work, oversaw the entire study including the work in the coordinating labs, contributed to the drafting of the work and gave final approval of the version to be published.

Statement of Ethics: All animal work was reviewed and approved by the NC State Institute of Animal Care and Use Committee (IACUC; approval number 20-150) and supervised by the attending veterinarian. All animal work conformed to all applicable federal and state US laws.

Conflict of Interest Statement: The authors have no known or perceived conflicts of interest.

examined in developmental neurotoxicity studies. Pups were gestationally exposed via oral dosing to the dam to FM 550 or the BFR or OPFR components at environmentally relevant doses.

Results: The neonatal cortex was highly sexually dimorphic in lipid and transcriptome composition, and males were more significantly impacted by FR exposure. Multiple adverse modes of action for the BFRs and OPFRs on neurodevelopment were identified, with the OPFRs more disruptive than the BFRs via multiple mechanisms including dysregulation of mitochondrial function and disruption of cholinergic and glutamatergic systems. Disrupted mitochondrial function by environmental factors has been linked to higher risk of autism spectrum disorders. Impacted lipid classes included the ceramides, sphingomyelins, and triacylglycerides. Robust ceramide upregulation in the OPFR females could suggest heightened risk of brain metabolic disease.

Conclusions: This study reveals multiple mechanisms by which the components of a common FR mixture are developmentally neurotoxic and that the OPFRs may be the compounds of greatest concern.

Keywords

Lipidomics; transcriptomics; brain; TPP; THPH; ITPs IPP; developmental neurotoxicity; DNT; flame retardants; environmental toxicology; choline

INTRODUCTION

Chemical flame retardants (FR) are applied to a myriad of consumer products to comply with flammability standards aimed at delaying the spread of fire. Due to continued widespread use, FRs are prevalent pollutants in the natural and human environment including house dust and food sources (1–3). This is concerning because multiple FRs are thought to be neurotoxic and endocrine disrupting (4–6). In response to these toxicological concerns, over the last two decades the FR landscape has changed considerably with some phasing out and others phasing in. Most significantly, use of some polybrominated diphenyl ethers (PBDEs) was discontinued after being identified as thyroid disrupting and linked to deficits in memory and cognitive function (7). Since the PBDE phaseout, different brominated FRs (BFRs), sometimes called novel brominated FRs and other alternative FRs, have been developed and implemented as replacements (8, 9). Also, use of organophosphate esters (OPEs) as FRs (OPFRs) has rapidly grown in popularity largely because of their relatively rapid metabolism and assumed lower human toxicity; although that presumption of greater safety has been questioned (10–13). Notably, some OPEs have also been used in a variety of industrial applications for decades prior to their adoption as FRs, so global production was already high and human exposure widespread (14). The newer BFRs and OPFRs present in commercial mixtures such as FireMaster 550 (FM 550) were designed to be less neurotoxic than their predecessors, yet their potential to disrupt neurodevelopment has not been thoroughly investigated. Here, we utilized a combination of transcriptomic and lipidomic approaches to understand how exposure to these “next generation” FRs impacts neurodevelopment in Wistar rats of both sexes.

Commercially available FRs are often mixtures, sometimes containing both BFR and OPFR components. FM 550 is one such mixture that has been used since the early 2000s as an additive to treat foam-based furniture, baby products, and car seats among other common items (15, 16). FM 550 is composed of two brominated compounds, 2-ethylhexyl-2,3,4,5-tetrabromobenzoate (EH-TBB) and bis(2-ethylhexyl) 2,3,4,5-tetrabromophthalate (BEH-TEBP), the OPE triphenyl phosphate (TPHP), and numerous isopropylated triarylphosphate isomers (ITPs) (17, 18). FM 550 components can readily escape from products and multiple studies have demonstrated environmental mobility, persistence, and bioaccumulation (2, 19). Indoors, this includes contamination of house dust (1, 20, 21), where inhalation or ingestion is the most significant route of human exposure, especially for children (14). Higher levels of FM 550 components are regularly found in children compared to adults, likely due to increased hand-mouth behavior (22–24). In humans, OPFRs are metabolized more quickly than BFRs leading some to conclude they are, consequently, less likely to result in fetal exposure or toxicity (25, 26). We and others, however, have detected them in animal and human placenta, along with evidence of placental stress and other biomarkers of disrupted placental function (27–31).

Evidence of OPFR neurotoxicity is also growing (10, 11, 32, 33). Of additional concern is that human OPFR exposure is now on par with, or even higher than, historical PBDE peak exposure levels (10). Although the OPEs used as FRs were designed to have limited capacity to inhibit acetylcholine esterase, the primary mode of action by which the structurally similar OP pesticides have long been recognized to be neurotoxic, emerging evidence suggests they can still disrupt cholinergic and other neurotransmitter signaling pathways including cholinergic neurodifferentiation (12, 33, 34). Despite their widespread use, proper risk assessment of OPFRs and the newer BFRs has yet to be conducted.

To date, we and others have shown in a variety of experimental models that FM 550 is disruptive of sexually dimorphic socioemotional behaviors (27, 35, 36) and their related neural pathways (27, 29, 30, 32, 36–42). Less is known, however, about how each of the chemical classes may be contributing to those adverse outcomes. In a related, prior study using Wistar rats, we explored how perinatal exposure to FM 550 or its component classes alter a suite of behaviors in both sexes as adults (36). The animals were gestationally exposed to 1000 μg of the BFR mixture, 1000 μg of the OPFR mixture or 2000 μg FM 550 (36) via oral intake by the dam. We demonstrated that both the BFRs and the OPFRs can induce adverse behavioral outcomes, albeit differently, suggesting each class impacts the brain via different modes of action.

The present studies were conducted to further understand the underlying mechanisms driving these differences and identify unique outcomes of exposure to the full FM 550 mixture. Based on previous work in rodents demonstrating dysregulated neurodevelopment of the fetal forebrain (29, 30) and behavioral deficits (27, 36) following gestational exposure to FM550 and OPFRs, we chose to focus on the prefrontal cortex. Using postnatal day (PND) 1 cortices from siblings of the animals used for our previously published behavioral study (36), we employed a combination of transcriptomics, lipidomics, and validating PCR approaches to determine the possible pathways each chemical class disrupts. While transcriptomics is commonly utilized in exposure studies, lipidomics studies and combined

multi-omic evaluations are rare due to the complexity of lipidomics measurements (e.g., numerous lipid isomers and large dynamic range). However, since lipids constitute a major structural component of brain tissue and are involved in numerous signaling and biochemical processes, assessing how specific lipid species change in response to exposure is a potentially powerful method of assessing developmental neurotoxicity. Here we combined new analytical techniques to provide an in-depth lipid analyses of the species affected by environmental exposure in the developing brain (43). Collectively, our analyses explored how FM 550 and its component classes altered cortical lipid composition in combination with transcriptomics, to better understand molecular and structural perturbations associated with behavioral and cognitive deficits observed in prior studies.

In addition to its disruptive effects on sexually dimorphic socioemotional behaviors, FM 550 and its components have been found to be endocrine disrupting (44), disruptive of embryonic neural pathways (29, 30), and adipogenic with compromised bone composition a potentially consequential outcome (45, 46). Thus, we anticipated significantly altered pathways and genes, including peroxisome proliferator-activated receptors (PPARs) and their transcriptional partners, associated with these phenotypes. Given the rapidly emerging body of work demonstrating that OPFRs may not be as low risk as previously thought (11) this component class was of key interest.

MATERIALS AND METHODS

The ARRIVE (Animal Research: Reporting of In Vivo Experiments) Guidelines “Essential 10” Checklist for Reporting Animal Research was used in the construction of this manuscript with all elements met (47). The ARRIVE guidelines were developed in consultation with the scientific community as part of an NC3Rs (National Centre for the Replacement Refinement and Reduction of Animals in Research) initiative to improve the standard of reporting of research using animals.

Animals:

All animals were siblings of animals used for a previously published study (36). Animal care, maintenance and experimental protocols met the standards of the Animal Welfare Act and the U.S. Department of Health and Human Services ‘Guide for the Care and use of Laboratory Animals’ and were approved by the North Carolina State University (NCSU) Institutional Animal Care and Use Committee (IACUC; approval number 20-150). All procedures were approved and monitored by a supervising veterinarian throughout the duration of the project. Wistar rats were obtained from Charles River (Raleigh, NC) and/or bred in house as indicated in humidity- and temperature-controlled rooms, each with 12-h:12-h light:dark cycles at 25°C and 45–60% average humidity in the AAALAC approved Biological Resource Facility at NCSU. As in our prior studies (48, 49), and in accordance with recommended practices for endocrine disrupting chemical (EDC) research, all animals were housed in conditions specifically designed to minimize unintended EDC exposure including use of glass water bottles with metal sippers, soy free diet, woodchip bedding, and thoroughly washed polysulfone caging (50–52). Animals were generated from breeding adult naive Wistar rats obtained from Charles River (Raleigh, NC; 56 females at

PND 72 and 16 males at PND 90) maintained on Teklad 2020 (phytoestrogen-free) diet. Dams were weighed and randomly assigned to the four treatment groups (control, BFR, OPFR and FM 550) with average weight per group equaling approximately 300g (mean and standard deviation for each group: control 295 ± 16; BFR 301 ± 13; OPFR 293 ± 14; FM550 299 ± 12).

Dosing Prep:

All animals were orally dosed using concentrated solutions of FM 550, BFR or OPFR as previously described (36). Exposure concentrations were based on previous work demonstrating transplacental/lactational transfer, bioaccumulation, and neurotoxicity at levels lower than the purported NOAEL for the BFR mixture (27, 28, 30, 44). A concentration of 1000 μg/day was chosen for the BFR and OPFR groups to represent the approximate concentration of BFRs and OPFRs in the 2000 μg/day FM 550 dose (21, 53). All mixtures were prepared in Dr. Heather Stapleton's lab at Duke University. Dosing was not done blinded because the FM 550 mixture was a larger volume, and the control animals were always dose first to minimize risk of cross-contamination. The individual who did the dosing was not the same as the individual conducting the experiments to ensure experimental blinding. The FM 550 commercial mixture was obtained from Great Lakes Chemical (West Lafayette, Indiana) and a 50 mg/mL dosing solution was prepared by diluting the appropriate amount of FM 550 into sesame oil. The Stapleton lab also prepared the BFR and OPFR mixtures into working 50 mg/mL solutions. The OPFR mixture is the same as previously reported (30, 53) and included organic components of TPHP and isopropylated triphenyl phosphates (ITPs; also abbreviated IPPs). The FM 550 brominated component mixture (BFR) contained 2-ethylhexyl-2,3,4,5-tetrabromobenzoate (EH-TBB) and bis (2-ethylhexyl)-2,3,4,5-tetrabromophthalate (BEH-TEBP). Each dosing solution (sesame oil vehicle, 1000 μg/day BFR, 1000 μg/day OPFR, and 2000 μg/day FM 550) was stored in foil wrapped scintillation vials at 4°C.

Exposure:

Dam exposure was once per day, orally via a food treat as previously described (36), beginning 72 hours after pairing and continuing through PND1. All animals were presumed pregnant by 72 hours. The dams gave birth within three days of each other, an observation that supports this presumption. The oral dosing method was chosen to reduce handling and, consequently, possibly confounding prenatal stress (54). As previously reported (29), dosing was based on average group body weights (bw) of 300 g before they were impregnated; producing exposures of approximately 3.3 mg/kg bw/day BFR or OPFR and 6.6 mg/kg bw per day FM 550. Relative exposure likely decreased slightly across gestation as body weight increased (54). We elected not to adjust for weight gain across gestation to minimize animal handling. We concluded that the benefits of making small adjustments to dosing to account for increasing dam weight would not outweigh the risk of prenatal stress daily weighing could induce.

Tissue Collection and Cortical Isolation:

Parturition checks were done in the morning at the time of dosing and the first day a litter was present was designated PND0. On PND1, pups were euthanized via rapid decapitation

four hours after dosing (13:00 h ± 60 min) to control for time post-exposure and time of collection. Whole neonatal heads were collected, flash frozen, and stored at −80°C. To verify offspring sex, a single paw was collected, and PCR performed for sry as previously described (27, 55). Once sex was verified, 6 male and 6 female PND1 whole heads per exposure group were selected. For all compounds only one pup per sex (littermates in most cases) per litter were used (litter is the experimental unit). The OPFR group only had 5 females because of limited litter availability.

Similar to our previous work (56, 57), the whole heads were first cryosectioned at 20 μm (Leica CM 1900) from the most anterior portion of the cortex and the forebrain portion of the sequential sections collected with a brush (Figure 1), transferred to an Eppendorf tube, and stored at −80°C for RNA extraction and sequencing. Anatomical landmarks were identified using The Developing Rat Nervous System (58). For transcriptomics, forebrain tissue was collected from the regions depicted on P0 coronal plates 212–216. Anterior landmarks included clear separation of cortex and olfactory bulb and collection stopped on plate 216 as identified by the position of the corpus collosum, fornix and lateral ventricle. A 1.25 mm width by 1-1.15 mm deep micropunch was then used to isolate the medial portion of the cortex for lipidomics. These isolated tissues represent plates 216 – 221. Prior, pilot work established the smallest amount of tissue we could use for each approach and still obtain robust data. The transcriptomics and lipidomics tissues were taken sequentially to obtain sufficient tissue amounts while maximizing anatomical specificity to the degree possible. Moreover, while transcription is subregion and even cell specific (here we focused on the prefrontal region of cortex), lipid content is more regionally homogeneous. Thus, the lipid composition observed likely also applies to other cortical regions, including the prefrontal cortex.

RNA Extraction and Sequencing:

RNA extraction was performed with the Qiagen RNEasy Miniprep kit according to the manufacturer protocol (Qiagen, Cat. 74134). RNA quality was determined using an Agilent 2100 Bioanalyzer and all samples were found to have RNA integrity numbers (RIN) ≥ 9.2. Sequencing libraries were prepared as described previously (59) by the NC State Genome Science Lab (GSL), using NEBNext Ultra Directional RNA Library Prep kit and NEBNext Poly(A) mRNA Magnetic Isolation Module (catalogs E7420 and E7490; New England Biolabs, Ipswich, MA, USA) for Illumina sequencing. Isolation, heat fragmentation and priming were performed according to manufacturer instructions. cDNA synthesis was followed by purification and size selection. Finally, library clean-up was performed used AMPure XP beads (Beckman Coulter Genomics, Brea, CA, USA; Cat. A63881) and quality was assessed using the Agilent 2100 Bioanalyzer. For each sample, library sequencing was performed using a 50-bp paired-end protocol on a single lane of an NovaSeq6000 sequencer. Approximately, 50 to 90 million uniquely mapped reads were generated per fetal forebrain library. The raw data were deposited in NCBI's Gene Expression Omnibus (*the ID will be placed here upon manuscript acceptance*).

RNA-seq Data Processing and Analyses:

Quality control of read data was evaluated with FastQC. We used Cutadapt to trim sequences associated with library indexes, then alignment was performed using STAR short read aligner (60) to *Rattus norvegicus* (rn6) reference genome. The number of reads mapped to GENCODE was determined using featureCounts software. PCA plots and heatmaps were generated using the 500 most variable genes to assess data quality. It was observed that a small number of disproportionally over-expressed genes were potentially driving 11 samples to be outliers. To further examine this phenomenon, a heatmap of the top 50 expressed genes was created (Supplemental Figure S1a). Additional details of each gene ID listed in the heatmap was generated using Uniport (www.uniport.org) including gene symbol, full gene name and function. The NCBI database (www.ncbi.nlm.nih.gov) was then used to confirm presence and/or absence of those genes in neuronal tissue using RPKM data (Supplemental Table S1a). The primary tissue sources of some of the 50 genes in question were blood, hair, muscle, eye, skin, and bone, but not brain. Because the forebrain tissue was collected from whole head cryosections using a brush, risk of contamination by small amounts of ectopic tissue, particularly bone and eye, from sticking to the brush or the brain tissue as it was isolated is plausible. Based on this analysis and in consultation with a bioinformatician, rather than excluding the 11 samples, 13 genes expressed in bone and 19 genes expressed in eye were removed from the differentially expressed gene (DEG) set prior to data analysis (Supplemental Table S1b) to minimize analytical bias from ectopic expression. Additionally, because the PCA plots for the DEGs revealed clear separation by sex (Supplemental Figure S1b), the data were analyzed within sex to account for sex-specific effects.

Transcriptomics and Pathways Analysis—The goal of the approach was to probe for potential for sex-specific vulnerabilities and directional (up- or down-regulated) effects across exposure groups. Dispersion was estimated using DESeq2 Bioconductor package in the R statistical computing environment to normalize count data, estimate dispersion and fit a negative binomial model for each gene. The overall mean of the normalized counts, the log2 (fold-change), the *P* value and the adjusted *P* value (padj) were used to identify DEGs. Pathway analysis was then performed on each exposure group's up- and downregulated DEGs with padj < 0.05. Pathway analysis was performed with the online tool Enrichr using the modules for GO Biological Processes, Predicted Protein-Protein Interaction Hub Proteins (PPI), and KEGG.

RNAseq Validation using NanoString—To validate the RNAseq analysis and test predicted hub PPIs, a subfraction of each RNA extraction was also analyzed using the NanoString nCounter Analysis System (NanoString Technologies, Seattle, WA), which detects multiplexed gene targets without amplification or reverse transcription (61, 62). Genes were selected based on the results of the pathway analyses including the PPI (see Table S1 for selection details). In total, the code set included 29 up- or downregulated DEGs and 16 PPIs as well as 6 positive and 8 negative controls and 7 housekeeping genes for quality assurance (Table S2). Samples were normalized to 20 ng/μL prior to hybridization according to the manufacturer's instructions. Briefly, a master mix was created using 70 μL of hybridization buffer into the reporter code-set tube. For each individual sample, 8 μL of master mix, 5 μL of RNA sample and 2 μL of capture probe-set was added to NanoString

strip tubes and allowed to hybridize at 65°C for 20 hours in a thermal cycler. Following hybridization, all samples were run on the NanoString nCounter Max Analysis System. The nCounter Prep Station incubation time was set to high sensitivity and nCounter Digital Analyzer set to max count.

Lipidomics:

Lipid Extraction—Lipids were isolated from cortical micropunches using a modified Folch extraction (63, 64). Cortical tissue was combined with 750 μL of −20°C methanol and homogenized in 2.0 mL, 2.4 mm tungsten-carbine bead tubes for 5 min with a Fisherbrand 24 bead mill. Samples were then transferred to Fisherbrand glass culture tubes containing another 750 μL of −20°C methanol where 3 mL of chloroform and 200 μL of water were added. The samples were then vortexed for 30 s, sonicated for 30 min, vortexed again for 30 s, and incubated for 1 h at 4°C. Following incubation 1.2 mL of water was added and samples were centrifuged for 10 min at 1000 x g. A 300 μL aliquot of the bottom lipid layer was finally transferred to a Sorenson microcentrifuge tube and dried *in vacuo.* The dried lipids were reconstituted in 190 μL of −20°C methanol and 10 μL of chloroform and then stored at −20°C until analysis with liquid chromatography, ion mobility spectrometry, collision induced dissociation and mass spectrometry (LC-IMS-CID-MS).

LC-IMS-CID-MS Analysis—The cortical lipid extracts were evaluated using an Agilent 1290 UPLC coupled to an Agilent 6560 IM-QTOF platform (Santa Clara, CA) with a commercial gas kit and MKS Instruments precision flow controller (Andover, MA). Lipids were first separated by reversed-phase LC by injecting 10 μL onto a Waters (Milford, MA) CSH column (3.0 mm x 150 mm x 1.7 μm particle size). The 34-minute gradient having a flow rate of 250 μL/min and mobile phase A of 10 mM ammonium acetate in 40:60 LC-MS grade acetonitrile/water and mobile phase B of 10 mM ammonium acetate in 90:10 LC-MS grade isopropanol/acetonitrile is detailed in (Table S3). Both positive and negative mode ESI analyses were performed on all samples. Following electrospray ionization (ESI), the ions were analyzed using the Agilent 6560 IM-QTOF MS platform (65, 66). Collision cross section were collected for all features detected and collision induced dissociation (CID) was performed with high purity nitrogen by ramping collision energies based on the ion arrival times analogous to previous IMS experiments (43, 67, 68). Alternating scans of no fragmentation and all-ions data independent acquisition (DIA) were used to collect precursor and fragmentation information at 1 sec/spectra for a mass range of 50-1700 *m/z.* All lipidomic raw data for this analysis is deposited and available in MassIVE (X).

Lipid Annotations—Spectra were annotated in Skyline by matching features to an in-house lipid library of 778 lipids with experimentally determined LC, IMS, MS and MS/MS information (69–72). Lipid annotations were made based on LC retention time, IMS collisional cross section, and *m/z* tolerances for precursor and fragment ions. The mass errors for all precursor annotations were <2 ppm and fragment mass error were <10 ppm. LC elution times were within 2 seconds of predicted elution times derived from Skyline's iRT feature and experimental collisional cross sections were within 1% of the library values. Using our LC-IMS-CID-MS platform enables the annotation of lipid fatty acyl and head group moieties but fatty acyl back bone attachment to the *sn-1* or *sn-2* positions, and double

bond orientations and placement are not differentiable with this platform and method (73). To elaborate, lipids were annotated with "_" to denote ambiguous fatty acyl positions and "/" when stereochemistry is known (e.g., PC(0:0_18:0) *versus* PC(0:0/18:0) or PC(18:0/0:0)). Lipids were also annotated with "a" or "b" to denote potential isomers. Additionally, features with multiple potential lipid matches are noted with ";" (e.g., PC(18:1_16:0); PC (18:0_16:1)). Lipids were also assigned annotations for their summed carbon and double bond number when individual fatty acyl information could not be obtained or annotated (e.g., PE(34:1)). Finally, peak areas of all annotated lipids were exported from Skyline for further processing and statistical analysis.

Lipidomics Statistical Analysis and Interpretation—The peak areas were transformed to a $\log_2$ scale and normalized against their total ion current (TIC) since tissue variability was possible. Samples were screened for potential outliers through analysis of the PAV-RMD algorithm (74), Pearson's correlation and principle component analysis using the *pmartR* (75) package in R (76) (Version 4.0.3 Vienna, Austria). Analysis of covariance (ANCOVA) was conducted to assess whether exposure influenced lipid abundances by comparing mean lipid peak areas of the control group to the exposed groups while accounting for differences in sex. Planned comparisons were implemented to compare control group lipid abundances to each of the exposed groups (BFR, OPFR or FM 550) separately and determine whether each lipid had a statistically significant fold change. Holm's correction was used to adjust *p*-values for multiple comparisons, and lipids having an adjusted $p \leq 0.05$ were considered statistically significant (77). Lipids were visualized using the SCOPE cheminformatics toolbox (78). In SCOPE, lipids were matched to the Lipid Maps Database to derive SMILES from which the ECFP6 fingerprints were calculated using the *rcdk* R package (79–82). Hierarchical clustering of molecular fingerprints utilizing Euclidean distances and average linkages were calculated using the *phangorn* R package, and heatmaps were plotted with the *ggtree* R package (83, 84). The resulting SCOPE dendrograms enabled visualization of the comparisons between the control and different exposure groups (BFR, OPFR or FM 550).

RESULTS

Litter Composition:

Details of dam and offspring body weights, maternal care and litter composition are reported in Witchey et al 2020. Briefly, dam body weights and maternal care did not differ across exposure groups at any time examined throughout the study. Although overall litter size did not differ across exposure groups, BFR dams had more female pups compared to controls. No significant differences were observed in offspring PND 1 body weights.

Transcriptomics:

For all compounds, the number of DEGs was greatest in males (Figure 2) with differential expression of 2633 FM 550, 2421 BFR, and 2858 OPFR genes at an adjusted p-value of <0.05. Affected numbers of DEGs were drastically fewer in female offspring: 7 FM 550, 2 BFR and 535 OPFR DEGs. To perform the pathway analyses, data were examined within sex and direction of change (up- or down-regulated). For the males, there were 1406, 1101,

and 1412 upregulated and 1168, 1276, and 1375 downregulated genes in FM 550, BFR and OPFR exposed groups respectively. Because so few genes were affected in the female FM 550 and BFR groups, pathway analysis was only performed on the OPFR female group, which consisted of 345 upregulated and 138 downregulated DEGs (Figure 2).

Pathway Analysis: Shared Expression Across Groups—Using the Ensembl IDs, to compare DEGs across groups, separate Venn diagrams were created for upregulated and downregulated genes within sex (https://bioinfogp.cnb.csic.es/tools/venny/) to identify overlapping DEGs. In males, 35% of the upregulated (703) and 30.1% of downregulated (629) genes were identified as DEGs in all three exposure groups (Figure 3). The FM 550 and BFR groups had 8.4% upregulated and 8.5% downregulated genes in common, while the FM 550 and OPFR groups had 13.7% upregulated and 6.8% downregulated genes in common. For the subsequent analysis, within each DEG subset (sex and direction), gene names were identified from the Ensembl IDs using the online tool Biodnet. Genes without names (unannotated regions) and genes for ribosomal proteins (rp) were removed from and excluded from pathways analysis. The modules in Enrichr used to identify enriched targets/pathways were Transcription Factor Protein-Protein Interaction (PPI), KEGG 2021 Human, and GO Biological Process 2021.

GO Biological Processes:

For the GO Biological process analyses, in males, there were 157 FM 550, 163 BFR and 180 OPFR upregulated and 24 FM 550, 42 BFR and 55 OPFR downregulated processes. In males, approximately 36% (92) of the upregulated and 26% (18) of the downregulated GO Biological processes were significantly altered across all three exposure groups (Supplemental Table S4). When comparing the top 10 upregulated and downregulated GO Biological pathways within each male exposure group, there were 5 and 4 consistently identified pathways respectively (Figure 4). The 5 upregulated were mRNA processing, RNA splicing via transesterification reactions, mRNA via spliceosome, mitochondrial ATP synthesis coupled electron transport and respiratory electron transport chain. The 4 downregulated were nervous system development, positive regulation of synaptic transmission, regulation of cationic channel activity and axonogenesis. When looking at unique GO Biological processes within exposure groups, OPFR exposure affected more GO processes related to mitochondrial function (13 upregulated) than BFR exposure (5 upregulated). BFR exposure uniquely produced effects on GO processes related to RNA replication including RNA polymerase 1 promotor (3 upregulated) and helicase activity (2 upregulated). The GO Biological processes specific to OPFR males were related to axon guidance/neuron growth (6 downregulated) and synaptic signaling (3 downregulated) (Table S5).

In the OPFR females, 16 GO Biological pathways were significantly upregulated. Of the 16, 11 were also identified in the OPFR-exposed males, 7 of which were related to mitochondrial regulation and in the top ten significantly altered pathways in males (Figure 4). No GO Biological pathways were significantly downregulated in the OPFR females.

Predicted Protein-Protein Interaction Hub Proteins:

In males, 24 FM 550, 31 BFR and 42 OPFR potential hub PPIs were identified for the upregulated DEGs, with 18 commonly predicted across all three groups. These were (in no specific order) ESR1, HTT, POU5F1, ILF3, ILF2, POLR2A, TARDBP, BRCA1, MYC, NANOG, RAD21, CTCF, TBP, TRIM28, TP53, UPF1, HSF1, PML. In the male downregulated DEG sets, only 1 FM 550, 3 BFR and no OPFR PPIs were identified. Downregulation of RXRA was predicted in both FM 550 and BFR exposed males (Table 1). No statistically significant PPIs were predicted for either the up- or downregulated DEGs in the OPFR females.

KEGG Pathways:

In males, 71% of upregulated KEGG pathways were shared across FM 550, BFR and OPFR exposed animals. Many of the 22 pathways common to all three were related to neuronal degenerative diseases including Huntington disease, Parkinson's disease, Alzheimer's disease, and oxidative phosphorylation (Figure 5A). Pathways unique to component class included ribosome biogenesis in eukaryotes and circadian rhythm for OPFR males and mitophagy for BFR males. There were also four KEGG pathways only observed to be upregulated in FM 550 males: nucleotide excision repair, pyrimidine metabolism, salmonella infection and shigellosis. By contrast, 2 FM 550, 4 BFR and 10 OPFR KEGG pathways were downregulated in males (Table S6). The only pathway shared between all male exposure groups was endocytosis. In the OPFR males, 8 KEGG pathways were exclusively downregulated including cholinergic and glutamatergic synapse and long-term depression.

In the OPFR females, there were 13 upregulated and 6 downregulated KEGG pathways. Twelve of the 13 upregulated KEGG pathways were also upregulated in OPFR-exposed males (Figure 5B). These were oxidative phosphorylation, Parkinson disease, thermogenesis, Prion disease, Huntington disease, diabetic cardiomyopathy, amyotrophic lateral sclerosis, non-alcoholic fatty liver disease, pathways of neurodegeneration, Alzheimer disease, retrograde endocannabinoid signaling, and cardiac muscle contraction. Two downregulated KEGG pathways were also common to both sexes: endocytosis and axon guidance.

Five upregulated KEGG pathways related to neurodegeneration were shared between all male exposures and OPFR females: Parkinson disease, Huntington disease, oxidative phosphorylation, Alzheimer's disease, and pathways of neurodegeneration. Within those KEGG pathways, 18 DEGs were commonly to all (Figure 5C). The majority of those shared genes are associated with cellular respiration including subunits of mitochondrial ATP synthase (ATP5), the terminal enzyme of the mitochondrial respiratory chain, cytochrome c oxidase enzyme (COX), NADH:ubiquinone oxidoreductase subunits (NDUFA) important for oxidative phosphorylation system in mitochondria, and components of the Ubiquinol-Cytochrome C Reductase (UCQR) complex, which is part of the part of the mitochondrial electron transport chain.

Transcriptomics Validation:

NanoString was used to validate aspects of the transcriptional data including 19 upregulated genes, 10 downregulated genes, and 16 predicted PPIs (Table S1). The average gene

expression count ranges were 5-92 for negative controls, 138-89, 160 for positive controls, and 836-4148 for housekeeping genes. The NanoString results were largely concordant with the RNAseq results and pathway analyses with some exceptions. Three genes of interest, POU5F1, OXTR and FOXP3, were found to have gene expression counts below those of the negative controls and thus considered not detected. This is not surprising since none are highly expressed in PND 1 cortex. Similarly, 4 upregulated DEGs (GNG5, Ndufa2, CLOCK, HTT), 1 downregulated DEG (CACNG) and 3 PPIs (ESR1, BRCA1 and RXRA) had expression levels below the lowest expressing housekeeping gene, Gusb, and were thus considered low expressors or undetected. These genes are also not highly expressed in developing cortex. Thus, confirmation of these PPIs would require examination of regions that more strongly express them. Full results are presented in Table S7.

Lipidomics Results—A total of 443 lipids (208 lipids in negative ion mode and 235 in positive) were identified from a target list of 778 lipids with LC-IMS-CID-MS. As illustrated in Figure 6A, the BFR-exposed pups had 29 significantly disrupted lipids, while those exposed to OPFRs had 38. As expected, the FM 550 exposed pups had the most lipidomic changes with 76 statistically significant lipids. Of those, 16 were shared by all exposure groups, and the OPFR exposed group had more lipid dysregulation in common with the FM 550 exposed group. Further breakdown of the statistically significant lipids is shown in Table S8. The disrupted lipids were then clustered by structural similarity and saturation or unsaturation of the fatty acyl chains (Figure 6B). Saturated free fatty acids (FAs) and saturated triacylglycerols (TGs) were observed to be downregulated for all the FM 550 exposed pups and the OPFR exposed pups, albeit to a lesser extent. Additionally, several sphingolipids, a lipid class including ceramides (Cers) and sphingomyelins (SMs), were also affected by exposure. Interestingly, Cers were upregulated by all three exposures, whereas SMs were predominantly downregulated in only the FM 550 exposed group.

Analysis by sex revealed strong sex differences in cortical lipid composition and impacts of exposure. In the unexposed controls, females had 101 statistically significant lipids with lower abundances than the males and only 2 with higher abundances. A high degree of dichotomy was also observed between the exposure groups within sex (Figure 7 and Table S9). Specifically, while the BFRs did not show strong lipid class-based trends for either sex, OPFR exposure caused SMs to decrease more in males than females. Additionally, while the male pups did not show any Cer dysregulation, many Cer species increased in the females in all three exposure groups. Both female and male rat pups also showed considerable Cer upregulation when exposed to FM 550, but only the males had substantial dysregulation of SMs. Both males and females in the FM 550 group had upregulation of unsaturated TGs and downregulation of saturated TGs, illustrating an exposure-based effect on double bond presence and absence for the fatty acyl groups in the lipids. When comparing commonalities between sexes for the BFR and OPFR exposed pups, there was very little overlap among the dysregulated lipids. Female and male pups therefore showed more dysregulation in common with respect to the whole FM 550 mixture as opposed to its individual components.

DISCUSSION

Both the transcriptomics and lipidomics analyses indicated that the OPFRs were the most biologically active component of the FM 550 mixture. Strong baseline sex differences were observed and, consequently, also highly sexually-dimorphic responses to prenatal FR exposure. Both component classes and the full FM 550 mixture appear capable of impairing aspects of mitochondrial function including oxidative phosphorylation, electron transport, and respiratory complex assembly and function. Mitochondrial dysfunction likely underlies the exposure-related identification of other pathways and systems, especially the numerous neurodegenerative pathways identified. Particularly in males, genes essential to mitochondrial function (ex. ATP5, COX, NDUF, UCQR) involving all but one of the electron chain complexes (Figure 8A), primarily drove neurodegenerative pathway enrichment. In males, OPFRs also downregulated KEGG pathways related to glutamatergic and cholinergic synapse function, and the synaptic vesicle cycle. Similarly, axon guidance and endocytosis were downregulated by OPFRs in both sexes, demonstrating that developmental neurotoxicity is multi-modal. The lipid analysis was largely concordant with the transcriptomics and indicative of sex-specific disruption of neurodevelopmental processes, especially myelination. Mitochondria are essential to support the energy-demanding nature of myelination, preserve membrane potential, and fuel the enormous amount of neural circuit reorganization and synaptic refinement that occurs postnatally (85, 86). Accordingly, mitochondrial dysfunction has been linked to many different pathological conditions of the developing central nervous system more common to boys including schizophrenia and autism spectrum disorders (ASD) (87, 88). Thus, the data generated herein support stated concerns that FRs, particularly OPFR, exposure contributes to greater risk of male-biased neurodevelopmental disorders (10, 89, 90).

The Significance of Sex Differences in Evaluating Exposure Outcomes

Profound sex differences in cortical lipid composition and transcriptome were identified at birth and, unsurprisingly, strongly sex-specific effects of exposure were also observed. That the perinatal period is a time of intense brain sexual dimorphism is well established (91, 92) and highly dependent on steroid hormones (93, 94). In rodents, testicular androgens, generated by a perinatal testicular hormone surge, are largely aromatized in the developing male brain and masculinize it via estrogen receptors (ERs), particularly the alpha form of ER (ERα) (95). In humans, although a similar androgen surge occurs in boys, brain masculinization requires androgen receptors, with ERs playing a vastly less significant role (96, 97). Thus, at birth, both rodent and human males have higher levels of circulating steroid hormones than females that drive brain sexual differentiation.

Accordingly, many transcripts and lipids with sexually dimorphic expression at birth are steroid sensitive, especially to estrogens (98). Significantly, at least one prior study using a combination of wildtype and ERα knockout mice found that OPFR exposure disrupts aspects of metabolic homeostasis with males displaying reduced energy intake and body weight but not ovariectomized females (99). Also reported, was that perinatal exposure to the same OPFR mixture (tris(1,3-dichloro-2-propyl)phosphate (TDCPP), TPHP, and tricresyl phosphate (TCP), each at 1 mg/kg) via oral exposure to the mouse dam (GD 7

– PND 14) resulted in upregulation of hypothalamic ERα expression on PND 14 in females but not males (100). This upregulation was not observed at birth. Hub PPI performed herein identified ESR1 as a possible upstream target for both the BFRs and the OPFRs, as well as the full mixture, an observation consistent with the published mouse data. This prediction is also concordant with evidence reported by our group and others using a variety of *in vitro* and *in vivo* models demonstrating that FM 550 and its components are estrogen disrupting and can bind ERs including ERα (29, 101, 102). However, our attempt via NanoString analysis to test if ERα expression was disrupted was unsuccessful because it is not highly expressed in the PND 1 rat cortex, thus it would have to be assessed elsewhere in the newborn brain.

Both brain RNA expression patterns and lipid composition, including mitochondrial lipid composition, are strongly sexually dimorphic at birth, with region-specific differences (103, 104). For example, cortical cardiolipin content is not dimorphic across early neonatal development but saturation is, with females having a higher saturation ratio at birth then dropping to male typical levels by PND 4 (105). This is strongly concordant with neonatal patterns of brain ER expression, which can be highly sexually dimorphic at birth, but rapidly change (106, 107). In the cortex, the cardiolipin biosynthetic pathway is sensitive to estrogens (108), as are many other nervous system lipids including endocannabinoids (109) and their metabolism (98). Critically, mitochondria are also highly sexually dimorphic with fatty acid utilization and functional capacities including electron transport capacity typically higher in adult female brain mitochondria than male brain mitochondria (110). Estrogens also profoundly alter mitochondrial biogenics via mechanisms involving both canonical ERs and GPER1 depending on age and tissue type (111).

Collectively, these brain structural and functional sexual dimorphisms likely underlie sex and region-specific vulnerabilities to neuropsychiatric disorders including ASD (112–114), and adverse outcomes to environmental insults including chemical exposures (115, 116). Here we found that the OPFRs in particular disrupted mitochondrial pathways in both sexes related to the respiratory electron transport chain, mitochondrial ATP synthesis, and NADH dehydrogenase complex assembly with the male groups also showing strong evidence of downregulated pathways associated with nervous system development, axonogenesis, synaptic transmission and both cholinergic and gluatamatergic synapse function, suggesting that male neurodevelopment is more sensitive to exposure and, potentially, the consequences of mitochondrial disruption. This is consistent with evidence that prenatal chemical exposures increase ASD risk by perturbing mitochondrial physiology (117).

FR Disruption of Mitochondrial Function

The BFRs and OPFRs both appear to have profound, albeit somewhat different, effects on mitochondrial function and, consequently, neurodevelopment, with the BFRs having a smaller sequala of effects than the OPFRs. Numerous mitochondrial GO processes were affected by both OPFR and FM 550 exposure (Table S10), including mitochondrial respiratory chain complex assembly (especially Complex I), indicating that the OPFRs are likely the primary drivers of FM 550 mitochondrial stress. Additionally, OPFR exposure exclusively affected 2 mitochondrial GO process: establishment of protein

localization to mitochondrial membrane (GO:0090151) and mitochondrial RNA metabolic process (GO:0000959). Our OPFR results are consistent with prior work in the nematode (*Caenorhabditis elegans*) led by the National Toxicology Program (NTP), which reported evidence of significant OPE-related mitochondrial toxicity, particularly for TPHP, BDHP and TMPP, with various degrees of cytotoxicity at higher doses (33). The authors concluded that OPFRs are comparable to PBDEs on mitochondrial toxicity. This is significant because PBDE exposure has been linked to heightened ASD risk (89), purportedly via mitochondrial toxicity (118).

By contrast, the BFRs primarily only affected GO processes related to mitochondrial ATP synthesis and electron transport, suggesting they may have a somewhat different mode of action on mitochondria than the OPFRs. BFRs were also linked to upregulated responses to hypoxia, and catabolic processes including ubiquitin-dependent protein catabolic processes. To at least some extent, thyroid hormones regulate maturation of brain mitochondria and the electron transport chain (119), and prenatal hypothyroidism has long been known to induce severe neurodevelopmental abnormalities (120). Many legacy BFRs, most notoriously the phased out PBDEs, impair thyroid signaling. Prior studies on the newer BFRs, however, have produced inconsistent results and collectively suggest that the thyroid-disrupting potential of the BFRs tested herein is minimal at best, particularly compared to the PBDEs (44, 121, 122).

FR Disruption of Neurotransmitter System Development

Upregulated KEGG pathways in both sexes and all exposure groups included numerous pathways related to neurodegeneration including Parkinson’s, Alzheimer’s, and Huntington diseases. While this may seem counterintuitive for a newborn brain, the DEGs shared across these pathways are strongly involved in the electron transport chain and oxidative phosphorylation (Figure 8). Thus, critically, the enrichment of neurodegenerative pathways in the FR exposure groups likely does not indicate that developmental exposure contributes to higher risk of later in life disorders such as Alzheimer’s Disease per say, but rather emphasizes the fundamental significance of mitochondrial health for nervous system health and cognitive development (for example see Figure 8B). Within the Alzheimer’s disease KEGG pathway, for example, exposure upregulated genes integral to four of the five electron transport chain complexes plus TUBB which is associated with axonal transport defects, demonstrating the importance of these genes for not only neurodegeneration but neurodevelopment. Finally, all FR groups produced evidence that fundamental processes such as those related to protein processing in the endoplasmic reticulum and RNA transport, were upregulated which also signifies neurodevelopmental disruption.

In the OPFR exposed animals, aspects of endocytosis were disrupted as well as pathways for long term depression (LTD) and vesicle, vacuolar and cytoplasmic vesicle membrane formation, suggesting disruption of neurotransmitter systems and function. Accordingly, downregulation of genes required for axon guidance was found in both sexes (Figure 9 A&B), as well as genes related to glutamatergic and cholinergic synapses specifically in males (Figure 9 C&D), including ACHE and CAM2KA. Downregulation of the axon guidance KEGG pathway by OPFRs (Figure 9B) is consistent with our prior observation

that prenatal exposure to OPFRs alters serotonergic innervation of the rat fetal forebrain (30). Critically, glutamate, the most prevalent neurotransmitter in the frontal cortex, is packaged and released from presynaptic vesicles. Glutamatergic neurons are capable of many different forms of LTD and thus many forms of neuroplasticity (123) one of which, endocannabinoid-dependent LTD, is common in the forebrain to both glutamatergic and GABAergic synapses, particularly in the prefrontal cortex (124). This form of synaptic plasticity can, among many things, modulate dopamine signaling and affect motivated behaviors including addiction. Forebrain cholinergic systems regulate behaviors including attention, habit formation, memory, motor activity and reward, and arise from neuronal precursors that could either become GABAergic or cholinergic, with most cholinergic cortical innervation occurring just after birth in the rat. Acetylcholine is critical for cortical refinement including dendrite stabilization, neuritogenesis and synaptogenesis (125). Mitochondria have an important role in supporting synaptic activity and the synthesis and packaging of some key neurotransmitters, including glutamate and choline (126, 127). Thus, generally, OPFRs appear capable via multiple mechanisms of altering vesicle-related synaptic activity including amino acid neurotransmitter packaging and release, and cortical organization and plasticity. Significantly, our results support prior work illustrating that OPEs, including TPHP, while perhaps not as capable of impacting acetylcholinesterase activity as their predecessors, impact other aspects of choline metabolism and signaling (128–130).

FRs and Neonatal Cortical Lipid Composition

A notable endpoint where the full mixture was more impactful than either component class was the exposure- and sex-dependent impact of Cer levels. While both the OPFRs and the BFRs upregulated certain ceramide species in females, Cer upregulation in males was only observed in the FM 550 group. This suggests that males may be more resilient to exposure of the individual FM 550 components, and the full mixture is needed to overcome this resilience and produce disruption. Similarly, SMs, which are derived from Cers, essential for myelin formation, and ubiquitous in cell membranes, were profoundly downregulated in FM 550 males with females seemingly more resistant.

Cers and SMs are intensely studied in the context of neurodegenerative disease because they are associated with Alzheimer’s disease and Multiple Sclerosis, but their roles in development are less well delineated. Interestingly, one rat study identified a transient dip in brain Cer levels at birth but did not account for sex (131). Similarly, sphingosine levels were shown to be markedly higher than dihydrosphingosine levels. Further work using a wider range of OPFR and BFR doses will be needed to more comprehensively explore the sex difference in Cer and SM sensitivity. However, the observation that dysregulation was so sex specific is compelling, especially since Cers are beneficial for the early growth and development of neuronal cells, and sphingolipids are critical components of cell membranes and potent signaling molecules in many pathophysiological processes including neuroinflammatory processes (132). Accumulation of brain Cers have also been implicated in energy balance disorders and, because de novo synthesis occurs in the smooth endoplasmic reticulum and the mitochondria, their disruption lends further support to the conclusion that FM 550, and the OPFRs in particular, disrupt mitochondrial function (133).

Cer concentrations are precisely controlled with cellular growth or death resulting from very slight shifts (134). Cers are highly sensitive to endogenous estrogens, and essential to key aspects of neural and synapse development including myelination (135). More work is needed to understand how brain Cer composition may be vulnerable to FR exposure and what the resulting consequences may be.

Another finding of interest from the lipidomic studies is the upregulation of TGs with unsaturated fatty acids and downregulation of TGs with saturated fatty acids for both the males and females exposed to FM 550. Saturated and unsaturated fatty acids are known to have different health effects and this split regulation indicates disruption of specific enzymatic activity occurring for the different TGs upon exposure of the FM 550 mixture. To our knowledge, no prior study has reported this split, likely because many fatty acid analyses are performed with gas chromatography coupled to mass spectrometry (GC-MS), which cleaves the fatty acyl groups from the lipid headgroups. This causes a pool of all fatty acids in the sample and ultimately the inability to distinguish specific lipid species trends. Therefore, we find this result quite novel and a unique benefit of our approach that we will follow up in future studies.

Disruption of Other Neurodevelopmental Mechanisms

A few of the GO processes associated with FM 550 or BFR exposure involved modulation of viral and related process. While this may at first appear odd, genes in this process include IGF2R and APOE, which have significant roles in embryonic development and neural function. APOE was downregulated in both the BFR and FM 550 males. APOE codes for Apolipoprotein E (ApoE) which is expressed at the surface of TG-rich lipoproteins, chylomicrons and very low density lipoproteins (VLDL), acting as a receptor binding ligand and is critical for lipid transport in the brain (136, 137). In humans there are multiple APOE alleles, with apoE4 conferring the strongest genetic risk factor for Alzheimer’s disease (138).

The hub PPI analysis predicted downregulation of RXRA for both FM 550 and the BFRs but not the OPFRs. RXRs are common binding partners to many other nuclear receptors, especially PPARs, liver X receptors (LXRs) and vitamin D receptors (VDRs). The PPI result is concordant with prior work in rat placenta identifying disruption of LXR/RXR pathways as a primary outcome of FM 550 exposure (29). Notably, the RXRA/PPARα heterodimer is required for PPARα transcriptional activity on fatty acid oxidation genes such as ACOX1 and the P450 system genes, and plays a significant role in oxidative stress, energy homeostasis, mitochondrial fatty acids metabolism and inflammation in the brain (139). Genes in the PPAR/RXR family are also involved in aspects of neural proliferation and differentiation, myelination, and synaptic plasticity, and have been associated with neurodevelopmental disorders including schizophrenia (140). Prior animal and in vitro studies suggest that FM 550 and the OPFRs, particularly TPHP and ITP, may have adipogenic effects via PPARγ activation and PPARγ-mediated aP2 enhancer activity (46, 101, 141). The combined effects of OPFR exposure on PPARγ-related targets and BFR exposure on LXR/LXR endpoints could possibly account for some unique and/or absence of effects by the FM 550 mixture.

CONCLUSIONS

FM 550 induced transcriptome and lipid dysregulation associated with both of its constituent chemical components. Collectively, the data revealed multiple adverse modes of action for the BFRs and OPFRs on neurodevelopment. Most significantly, both induced mitochondrial disruption, which is associated with numerous neurodevelopmental disorders including ASD. The OPFRs were most disruptive, and via multiple mechanisms including dysregulation of mitochondrial function and disruption of cholinergic and glutamatergic systems. The discovery that the lipid composition of the PND1 cortex is so highly sexually dimorphic provides additional and novel insight as to how and why the male and female brain responds differently to environmental and other exogenous exposures and stresses. That pups of both sexes showed more lipid dysregulation in common with respect to the FM 550 mixture than its individual components indicate that exposure to the different FR classes affects the sexes differently on a molecular level. Lipid classes with the most notable changes included the ceramides, sphingomyelins, and triacylglycerides. Since dysregulated Cers are strongly associated with Alzheimer's disease risk, the robust upregulation of Cers observed in the OPFR exposed females could suggest heightened risk of brain metabolic disease at a very early age. Downregulation of phosphatidylcholines has also been noted in Alzheimer's disease due to choline shuttling, and downregulation was observed herein in pups exposed to OPFRs and the FM 550 mixture. Finally, this work emphasizes how essential it is that future studies regarding the impact of FRs and other exposures on neurodevelopment focus on sex differences. Too many resources and published studies remain either highly male biased or sex-agnostic (142).

Supplementary Material

Refer to Web version on PubMed Central for supplementary material.

Acknowledgements:

The authors are grateful to Heather Stapleton, with whom we have collaborated for years, for preparing the dosing mixtures, as well as David (Andy) Baltzegar, Director of the Genome Science Lab at NC State, for transcriptomics design consultation, library prep, and RNA sequencing. We also thank the staff in the Biological Resources Facility for their assistance with animal care and husbandry. All lipidomic measurements were performed in the Molecular Education, Technology and Research Innovation Center (METRIC) at NC State University.

Funding:

This work was supported by RO1ES028110 to HBP, U01ES026717 to DLA and P30ES0251278 to Rob Smart. MGD, MTO and ESB were supported by P42 ES027704 and P42 ES031009 and a cooperative agreement with the United States Environmental Protection Agency (STAR RD 84003201).

Data Availability Statement:

All data generated or analyzed during this study are included in this article, supplemental materials and the GEO and MassIVE repositories. Further enquiries can be directed to the corresponding author. *All raw transcriptomics data will be placed in a repository (GEO or similar) and all lipidomics data will be placed in MassIVE upon manuscript acceptance. Additionally, the repository names and reference numbers will be placed here and in the* Methods *section*.

REFERENCES

1. Dodson RE, Perovich LJ, Covaci A, Van den Eede N, lonas AC, Dirtu AC, et al. After the PBDE phase-out: a broad suite of flame retardants in repeat house dust samples from California. Environmental science & technology. 2012;46(24):13056–66. [PubMed: 23185960]
2. Ma Y, Venier M, Hites RA. 2-Ethylhexyl Tetrabromobenzoate and Bis(2-ethylhexyl) Tetrabromophthalate Flame Retardants in the Great Lakes Atmosphere. Environmental Science & Technology. 2012;46(1):204–8. [PubMed: 22128844]
3. Li J, Zhao L, Letcher RJ, Zhang Y, Jian K, Zhang J, et al. A review on organophosphate Ester (OPE) flame retardants and plasticizers in foodstuffs: Levels, distribution, human dietary exposure, and future directions. Environ Int. 2019;127:35–51. [PubMed: 30901640]
4. Dishaw LV, Macaulay LJ, Roberts SC, Stapleton HM. Exposures, mechanisms, and impacts of endocrine-active flame retardants. Curr Opin Pharmacol. 2014;19:125–33. [PubMed: 25306433]
5. Gaylord A, Osborne G, Ghassabian A, Malits J, Attina T, Trasande L. Trends in neurodevelopmental disability burden due to early life chemical exposure in the USA from 2001 to 2016: A population-based disease burden and cost analysis. Mol Cell Endocrinol. 2020;502:110666. [PubMed: 31952890]
6. Roze E, Meijer L, Bakker A, Van Braeckel KNJA, Sauer PJJ, Bos AF. Prenatal exposure to organohalogens, including brominated flame retardants, influences motor, cognitive, and behavioral performance at school age. Environ Health Perspect. 2009;117(12):1953–8. [PubMed: 20049217]
7. Costa LG, de Laat R, Tagliaferri S, Pellacani C. A mechanistic view of polybrominated diphenyl ether (PBDE) developmental neurotoxicity. Toxicol Lett. 2014;230(2):282–94. [PubMed: 24270005]
8. Hou R, Lin L, Li H, Liu S, Xu X, Xu Y, et al. Occurrence, bioaccumulation, fate, and risk assessment of novel brominated flame retardants (NBFRs) in aquatic environments - A critical review. Water Res. 2021;198:117168. [PubMed: 33962238]
9. Dong L, Wang S, Qu J, You H, Liu D. New understanding of novel brominated flame retardants (NBFRs): Neuro(endocrine) toxicity. Ecotoxicol Environ Saf. 2021;208:111570. [PubMed: 33396099]
10. Blum A, Behl M, Birnbaum L, Diamond ML, Phillips A, Singla V, et al. Organophosphate Ester Flame Retardants: Are They a Regrettable Substitution for Polybrominated Diphenyl Ethers? Environ Sci Technol Lett. 2019;6(11):638–49. [PubMed: 32494578]
11. Patisaul HB, Behl M, Birnbaum LS, Blum A, Diamond ML, Rojello Fernandez S, et al. Beyond Cholinesterase Inhibition: Developmental Neurotoxicity of Organophosphate Ester Flame Retardants and Plasticizers. Environ Health Perspect. 2021;129(10):105001. [PubMed: 34612677]
12. Behl M, Hsieh J-H, Shafer TJ, Mundy WR, Rice JR, Boyd WA, et al. Use of alternative assays to identify and prioritize organophosphorus flame retardants for potential developmental and neurotoxicity. Neurotoxicol Teratol. 2015;52:181–93. [PubMed: 26386178]
13. Hendriks HS, Westerink RH. Neurotoxicity and risk assessment of brominated and alternative flame retardants. Neurotoxicol Teratol. 2015;52(Pt B):248–69. [PubMed: 26363216]
14. Gbadamosi MR, Abdallah MA, Harrad S. A critical review of human exposure to organophosphate esters with a focus on dietary intake. Sci Total Environ. 2021;771:144752. [PubMed: 33540161]
15. Stapleton HM, Sharma S, Getzinger G, Ferguson PL, Gabriel M, Webster TF, et al. Novel and high volume use flame retardants in US couches reflective of the 2005 PentaBDE phase out. Environmental science & technology. 2012;46(24):13432–9. [PubMed: 23186002]
16. Stapleton HM, Klosterhaus S, Keller A, Ferguson PL, van Bergen S, Cooper E, et al. Identification of flame retardants in polyurethane foam collected from baby products. Environmental science & technology. 2011;45(12):5323–31. [PubMed: 21591615]
17. Stapleton HM, Misenheimer J, Hoffman K, Webster TF. Flame retardant associations between children's handwipes and house dust. Chemosphere. 2014;116:54–60. [PubMed: 24485814]
18. van der Veen I, de Boer J. Phosphorus flame retardants: properties, production, environmental occurrence, toxicity and analysis. Chemosphere. 2012;88(10):1119–53. [PubMed: 22537891]

19. Salamova A, Hermanson MH, Hites RA. Organophosphate and Halogenated Flame Retardants in Atmospheric Particles from a European Arctic Site. Environmental Science & Technology. 2014;48(11):6133–40. [PubMed: 24848787]

20. Stapleton HM, Allen JG, Kelly SM, Konstantinov A, Klosterhaus S, Watkins D, et al. Alternate and New Brominated Flame Retardants Detected in U.S. House Dust. Environmental Science & Technology. 2008;42(18):6910–6. [PubMed: 18853808]

21. van der Veen I, de Boer J. Phosphorus flame retardants: Properties, production, environmental occurrence, toxicity and analysis. Chemosphere. 2012;88(10):1119–53. [PubMed: 22537891]

22. Gibson EA, Stapleton HM, Calero L, Holmes D, Burke K, Martinez R, et al. Differential exposure to organophosphate flame retardants in mother-child pairs. Chemosphere. 2019;219:567–73. [PubMed: 30553217]

23. Butt CM, Hoffman K, Chen A, Lorenzo A, Congleton J, Stapleton HM. Regional comparison of organophosphate flame retardant (PFR) urinary metabolites and tetrabromobenzoic acid (TBBA) in mother-toddler pairs from California and New Jersey. Environ Int. 2016;94:627–34. [PubMed: 27397928]

24. Cowell WJ, Stapleton HM, Holmes D, Calero L, Tobon C, Perzanowski M, et al. Prevalence of historical and replacement brominated flame retardant chemicals in New York City homes. Emerg Contam. 2017;3(1):32–9. [PubMed: 28989983]

25. Roberts SC, Macaulay LJ, Stapleton HM. In vitro metabolism of the brominated flame retardants 2-ethylhexyl-2,3,4,5-tetrabromobenzoate (TBB) and bis(2-ethylhexyl) 2,3,4,5-tetrabromophthalate (TBPH) in human and rat tissues. Chem Res Toxicol. 2012;25(7):1435–41. [PubMed: 22575079]

26. Phillips AL, Herkert NJ, Ulrich JC, Hartman JH, Ruis MT, Cooper EM, et al. In Vitro Metabolism of Isopropylated and tert-Butylated Triarylphosphate Esters Using Human Liver Subcellular Fractions. Chem Res Toxicol. 2020;33(6):1428–41. [PubMed: 32129605]

27. Baldwin KR, Phillips AL, Horman B, Arambula SE, Rebuli ME, Stapleton HM, et al. Sex Specific Placental Accumulation and Behavioral Effects of Developmental Firemaster 550 Exposure in Wistar Rats. Sci Rep. 2017;7(1):7118. [PubMed: 28769031]

28. Phillips AL, Chen A, Rock KD, Horman B, Patisaul HB, Stapleton HM. Editor's Highlight: Transplacental and Lactational Transfer of Firemaster(R) 550 Components in Dosed Wistar Rats. Toxicol Sci. 2016;153(2):246–57. [PubMed: 27370412]

29. Rock KD, Horman B, Phillips AL, McRitchie SL, Watson S, Deese-Spruill J, et al. EDC IMPACT: Molecular effects of developmental FM 550 exposure in Wistar rat placenta and fetal forebrain. Endocrine connections. 2018;7(2):305–24. [PubMed: 29351906]

30. Rock KD, St Armour G, Horman B, Phillips A, Ruis M, Stewart AK, et al. Effects of Prenatal Exposure to a Mixture of Organophosphate Flame Retardants on Placental Gene Expression and Serotonergic Innervation in the Fetal Rat Brain. Toxicol Sci. 2020.

31. Varshavsky JR, Robinson JF, Zhou Y, Puckett KA, Kwan E, Buarpung S, et al. Organophosphate Flame Retardants, Highly Fluorinated Chemicals, and Biomarkers of Placental Development and Disease During Mid-Gestation. Toxicol Sci. 2021;181(2):215–28. [PubMed: 33677611]

32. Glazer L, Hawkey AB, Wells CN, Drastal M, Odamah KA, Behl M, et al. Developmental Exposure to Low Concentrations of Organophosphate Flame Retardants Causes Life-Long Behavioral Alterations in Zebrafish. Toxicol Sci. 2018;165(2):487–98. [PubMed: 29982741]

33. Behl M, Rice JR, Smith MV, Co CA, Bridge MF, Hsieh JH, et al. Editor's Highlight: Comparative Toxicity of Organophosphate Flame Retardants and Polybrominated Diphenyl Ethers to Caenorhabditis elegans. Toxicol Sci. 2016;154(2):241–52. [PubMed: 27566445]

34. Dishaw LV, Powers CM, Ryde IT, Roberts SC, Seidler FJ, Slotkin TA, et al. Is the PentaBDE replacement, tris (1,3-dichloro-2-propyl) phosphate (TDCPP), a developmental neurotoxicant? Studies in PC12 cells. Toxicol Appl Pharmacol. 2011;256(3):281–9. [PubMed: 21255595]

35. Gillera SEA, Marinello WP, Horman BM, Phillips AL, Ruis MT, Stapleton HM, et al. Sex-specific effects of perinatal FireMaster(R) 550 (FM 550) exposure on socioemotional behavior in prairie voles. Neurotoxicol Teratol. 2020;79:106840. [PubMed: 31730801]

36. Witchey SK, Al Samara L, Horman BM, Stapleton HM, Patisaul HB. Perinatal exposure to FireMaster(R) 550 (FM550), brominated or organophosphate flame retardants produces sex

and compound specific effects on adult Wistar rat socioemotional behavior. Horm Behav. 2020;126:104853. [PubMed: 32949556]

37. Slotkin TA, Skavicus S, Stapleton HM, Seidler FJ. Brominated and organophosphate flame retardants target different neurodevelopmental stages, characterized with embryonic neural stem cells and neuronotypic PC12 cells. Toxicology. 2017;390:32–42. [PubMed: 28851516]
38. Bailey JM, Levin ED. Neurotoxicity of FireMaster 550® in zebrafish (Danio rerio): Chronic developmental and acute adolescent exposures. Neurotoxicol Teratol. 2015;52(Pt B):210–9. [PubMed: 26239867]
39. Jarema KA, Hunter DL, Shaffer RM, Behl M, Padilla S. Acute and developmental behavioral effects of flame retardants and related chemicals in zebrafish. Neurotoxicol Teratol. 2015;52(Pt B):194–209. [PubMed: 26348672]
40. Quevedo C, Behl M, Ryan K, Paules RS, Alday A, Muriana A, et al. Detection and Prioritization of Developmental Neurotoxic and/or Neurotoxic Compounds Using Zebrafish. Toxicological sciences : an official journal of the Society of Toxicology. 2019;168(1):225–40. [PubMed: 30521027]
41. Guigueno MF, Karouna-Renier NK, Henry PFP, Peters LE, Palace VP, Letcher RJ, et al. Sex-specific responses in neuroanatomy of hatchling American kestrels in response to embryonic exposure to the flame retardants bis(2-ethylhexyl)-2,3,4,5-tetrabromophthalate and 2-ethylhexyl-2,3,4,5-tetrabromobenzoate. Environ Toxicol Chem. 2018;37(12):3032–40. [PubMed: 30035332]
42. Castorina R, Bradman A, Stapleton HM, Butt C, Avery D, Harley KG, et al. Current-use flame retardants: Maternal exposure and neurodevelopment in children of the CHAMACOS cohort. Chemosphere. 2017;189:574–80. [PubMed: 28963974]
43. Odenkirk MT, Horman BM, Dodds JN, Patisaul HB, Baker ES. Combining Micropunch Histology and Multidimensional Lipidomic Measurements for In-Depth Tissue Mapping. ACS Meas Sci Au. 2022;2(1):67–75. [PubMed: 35647605]
44. Patisaul HB, Roberts SC, Mabrey N, McCaffrey KA, Gear RB, Braun J, et al. Accumulation and endocrine disrupting effects of the flame retardant mixture Firemaster® 550 in rats: an exploratory assessment. J Biochem Mol Toxicol. 2013;27(2):124–36. [PubMed: 23139171]
45. Macari S, Rock KD, Santos MS, Lima VTM, Szawka RE, Moss J, et al. Developmental Exposure to the Flame Retardant Mixture Firemaster 550 Compromises Adult Bone Integrity in Male but not Female Rats. Int J Mol Sci. 2020;21(7).
46. Pillai HK, Fang M, Beglov D, Kozakov D, Vajda S, Stapleton HM, et al. Ligand binding and activation of PPARγ by Firemaster® 550: effects on adipogenesis and osteogenesis in vitro. Environ Health Perspect. 2014;122(11):1225–32. [PubMed: 25062436]
47. Kilkenny C, Browne WJ, Cuthill IC, Emerson M, Altman DG. Improving bioscience research reporting: the ARRIVE guidelines for reporting animal research. PLoS Biol. 2010;8(6):e1000412. [PubMed: 20613859]
48. Rock KD, Gillera SEA, Devarasetty P, Horman B, Knudsen G, Birnbaum LS, et al. Sex-specific behavioral effects following developmental exposure to tetrabromobisphenol A (TBBPA) in Wistar rats. Neurotoxicology. 2019;75:136–47. [PubMed: 31541695]
49. Patisaul HB, Adewale HB. Long-term effects of environmental endocrine disruptors on reproductive physiology and behavior. Frontiers in behavioral neuroscience. 2009;3:10-. [PubMed: 19587848]
50. Thigpen JE, Setchell KDR, Ahlmark KB, Locklear J, Spahr T, Caviness GF, et al. Phytoestrogen content of purified open- and closed-formula laboratory animal diets. Laboratory Animal Sciences. 1999;49(5):530–6.
51. Howdeshell KL, Peterman PH, Judy BM, Taylor JA, Orazio CE, Ruhlen RL, et al. Bisphenol A is released from used polycarbonate animal cages into water at room temperature. Environ Health Perspect. 2003;111(9):1180–7. [PubMed: 12842771]
52. Li AA, Baum MJ, McIntosh LJ, Day M, Liu F, Gray LE Jr. Building a scientific framework for studying hormonal effects on behavior and on the development of the sexually dimorphic nervous system. Neurotoxicology. 2008;29(3):504–19. [PubMed: 18502513]

53. Phillips AL, Hammel SC, Konstantinov A, Stapleton HM. Characterization of Individual Isopropylated and tert-Butylated Triarylphosphate (ITP and TBPP) Isomers in Several Commercial Flame Retardant Mixtures and House Dust Standard Reference Material SRM 2585. Environ Sci Technol. 2017;51(22):13443–9. [PubMed: 29076339]
54. Charil A, Laplante DP, Vaillancourt C, King S. Prenatal stress and brain development. Brain Res Rev. 2010;65(1):56–79. [PubMed: 20550950]
55. Poletti A, Celotti F, Rumio C, Rabuffetti M, Martini L. Identification of type 1 5alpha-reductase in myelin membranes of male and female rat brain. Mol Cell Endocrinol. 1997;129(2):181–90. [PubMed: 9202401]
56. Arambula SE, Belcher SM, Planchart A, Turner SD, Patisaul HB. Impact of Low Dose Oral Exposure to Bisphenol A (BPA) on the Neonatal Rat Hypothalamic and Hippocampal Transcriptome: A CLARITY-BPA Consortium Study. Endocrinology. 2016;157(10):3856–72. [PubMed: 27571134]
57. Arambula SE, Jima D, Patisaul HB. Prenatal bisphenol A (BPA) exposure alters the transcriptome of the neonate rat amygdala in a sex-specific manner: a CLARITY-BPA consortium study. Neurotoxicology. 2018;65:207–20. [PubMed: 29097150]
58. Paxinos G, Ashwell KW. Atlas of the developing rat nervous system: Academic Press; 2018.
59. Puzianowska-Kuznicka M, Pietrzak M, Turowska O, Nauman A. Thyroid hormones and their receptors in the regulation of cell proliferation. Acta Biochim Pol. 2006;53(4):641–50. [PubMed: 17115080]
60. Wise LM, Sadowski RN, Kim T, Willing J, Juraska JM. Long-term effects of adolescent exposure to bisphenol A on neuron and glia number in the rat prefrontal cortex: Differences between the sexes and cell type. Neurotoxicology. 2016;53:186–92. [PubMed: 26828634]
61. Brumbaugh CD, Kim HJ, Giovacchini M, Pourmand N. NanoStriDE: normalization and differential expression analysis of NanoString nCounter data. BMC Bioinformatics. 2011;12:479. [PubMed: 22177214]
62. Eastel JM, Lam KW, Lee NL, Lok WY, Tsang AHF, Pei XM, et al. Application of NanoString technologies in companion diagnostic development. Expert Rev Mol Diagn. 2019;19(7):591–8. [PubMed: 31164012]
63. Dittmar T, Koch B, Hertkorn N, Kattner G. A simple and efficient method for the solid-phase extraction of dissolved organic matter (SPE-DOM) from seawater. Limnology and Oceanography: Methods. 2008;6(6):230–5.
64. Nakayasu ES, Nicora CD, Sims AC, Burnum-Johnson KE, Kim YM, Kyle JE, et al. MPLEx: a Robust and Universal Protocol for Single-Sample Integrative Proteomic, Metabolomic, and Lipidomic Analyses. mSystems. 2016;1(3).
65. May JC, Goodwin CR, Lareau NM, Leaptrot KL, Morris CB, Kurulugama RT, et al. Conformational ordering of biomolecules in the gas phase: nitrogen collision cross sections measured on a prototype high resolution drift tube ion mobility-mass spectrometer. Anal Chem. 2014;86(4):2107–16. [PubMed: 24446877]
66. Abou-Elwafa Abdallah M. Environmental occurrence, analysis and human exposure to the flame retardant tetrabromobisphenol-A (TBBP-A)-A review. Environ Int. 2016;94:235–50. [PubMed: 27266836]
67. Becker C, Fernandez-Lima FA, Gillig KJ, Russell WK, Cologna SM, Russell DH. A novel approach to collision-induced dissociation (CID) for ion mobility-mass spectrometry experiments. J Am Soc Mass Spectrom. 2009;20(6):907–14. [PubMed: 19135385]
68. Baker ES, Tang K, Danielson WF 3rd, Prior DC, Smith RD. Simultaneous fragmentation of multiple ions using IMS drift time dependent collision energies. J Am Soc Mass Spectrom. 2008;19(3):411–9. [PubMed: 18226544]
69. Adams KJ, Pratt B, Bose N, Dubois LG, St John-Williams L, Perrott KM, et al. Skyline for Small Molecules: A Unifying Software Package for Quantitative Metabolomics. J Proteome Res. 2020;19(4):1447–58. [PubMed: 31984744]
70. MacLean B, Tomazela DM, Shulman N, Chambers M, Finney GL, Frewen B, et al. Skyline: an open source document editor for creating and analyzing targeted proteomics experiments. Bioinformatics. 2010;26(7):966–8. [PubMed: 20147306]

71. Kirkwood KI, Christopher MW, Burgess JL, Littau SR, Foster K, Richey K, et al. Development and Application of Multidimensional Lipid Libraries to Investigate Lipidomic Dysregulation Related to Smoke Inhalation Injury Severity. J Proteome Res. 2022;21(1):232–42. [PubMed: 34874736]
72. Kirkwood KI, Pratt BS, Shulman N, Tamura K, MacCoss MJ, MacLean BX, et al. Utilizing Skyline to analyze lipidomics data containing liquid chromatography, ion mobility spectrometry and mass spectrometry dimensions. Nature Protocols. 2022.
73. Koelmel JP, Ulmer CZ, Jones CM, Yost RA, Bowden JA. Common cases of improper lipid annotation using high-resolution tandem mass spectrometry data and corresponding limitations in biological interpretation. Biochim Biophys Acta Mol Cell Biol Lipids. 2017;1862(8):766–70. [PubMed: 28263877]
74. Matzke MM, Waters KM, Metz TO, Jacobs JM, Sims AC, Baric RS, et al. Improved quality control processing of peptide-centric LC-MS proteomics data. Bioinformatics. 2011 ;27(20):2866–72. [PubMed: 21852304]
75. Stratton KG, Webb-Robertson BM, McCue LA, Stanfill B, Claborne D, Godinez I, et al. pmartR: Quality Control and Statistics for Mass Spectrometry-Based Biological Data. J Proteome Res. 2019;18(3):1418–25. [PubMed: 30638385]
76. Team RC. R: A Language and Environment for Statistical Computing2013.
77. Holm S. A Simple Sequentially Rejective Multiple Test Procedure. Stat SJ, editor1979.
78. Odenkirk MT, Zin PPK, Ash JR, Reif DM, Fourches D, Baker ES. Structural-based connectivity and omic phenotype evaluations (SCOPE): a cheminformatics toolbox for investigating lipidomic changes in complex systems. Analyst. 2020;145(22):7197–209. [PubMed: 33094747]
79. Sud M, Fahy E, Cotter D, Brown A, Dennis EA, Glass CK, et al. LMSD: LIPID MAPS structure database. Nucleic Acids Res. 2007;35(Database issue):D527–32. [PubMed: 17098933]
80. Rogers D, Hahn M. Extended-connectivity fingerprints. J Chem Inf Model. 2010;50(5):742–54. [PubMed: 20426451]
81. Guha R. Chemical Informatics Functionality in R. J Stat Softw. 2007.
82. Weininger D. SMILES, a Chemical Language and Information System: 1: Introduction to Methodology and Encoding Rules. J Chem Inf Comput Sci 1988.
83. Schliep KP. phangorn: phylogenetic analysis in R. Bioinformatics. 2011;27(4):592–3. [PubMed: 21169378]
84. Yu GS DK; Zhu H; Guan Y; Lam TTY Ggtree: An r Package for Visualization and Annotation of Phylogenetic Trees with Their Covariates and Other Associated Data. Methods Ecol Evol. 2017.
85. Son G, Han J. Roles of mitochondria in neuronal development. BMB Rep. 2018;51(11):549–56. [PubMed: 30269744]
86. Khacho M, Slack RS. Mitochondrial dynamics in the regulation of neurogenesis: From development to the adult brain. Dev Dyn. 2018;247(1):47–53. [PubMed: 28643345]
87. Mahony C, O'Ryan C. Convergent Canonical Pathways in Autism Spectrum Disorder from Proteomic, Transcriptomic and DNA Methylation Data. Int J Mol Sci. 2021;22(19).
88. Rose S, Niyazov DM, Rossignol DA, Goldenthal M, Kahler SG, Frye RE. Clinical and Molecular Characteristics of Mitochondrial Dysfunction in Autism Spectrum Disorder. Mol Diagn Ther. 2018;22(5):571–93. [PubMed: 30039193]
89. Messer A. Mini-review: polybrominated diphenyl ether (PBDE) flame retardants as potential autism risk factors. Physiol Behav. 2010;100(3):245–9. [PubMed: 20100501]
90. Vuong AM, Yolton K, Cecil KM, Braun JM, Lanphear BP, Chen A. Flame retardants and neurodevelopment: An updated review of epidemiological literature. Curr Epidemiol Rep. 2020;7(4):220–36. [PubMed: 33409120]
91. Simerly RB. Wired for reproduction: organization and development of sexually dimorphic circuits in the mammalian forebrain. Annu Rev Neurosci. 2002;25:507–36. [PubMed: 12052919]
92. Giedd JN, Castellanos FX, Rajapakse JC, Vaituzis AC, Rapoport JL. Sexual dimorphism of the developing human brain. Prog Neuropsychopharmacol Bol Psychiatry. 1997;21(8):1185–201.
93. Schwarz JM, McCarthy MM. Cellular mechanisms of estradiol-mediated masculinization of the brain. J Steroid Biochem Mol Biol. 2008;109(3-5):300–6. [PubMed: 18430566]

94. McCarthy MM. A new view of sexual differentiation of mammalian brain. J Comp Physiol A Neuroethol Sens Neural Behav Physiol. 2020;206(3):369–78. [PubMed: 31705197]
95. McCarthy MM. Estradiol and the developing brain. Physiol Rev. 2008;88(1):91–124. [PubMed: 18195084]
96. Wallen K. Hormonal influences on sexually differentiated behavior in nonhuman primates. Front Neuroendocrinol. 2005;26(1):7–26. [PubMed: 15862182]
97. Puts D, Motta-Mena NV. Is human brain masculinization estrogen receptor-mediated? Reply to Luoto and Rantala. Horm Behav. 2018;97:3–4. [PubMed: 28818501]
98. Morselli E, Santos RS, Gao S, Ávalos Y, Criollo A, Palmer BF, et al. Impact of estrogens and estrogen receptor-α in brain lipid metabolism. Am J Physiol Endocrinol Metab. 2018;315(1):E7–e14. [PubMed: 29509437]
99. Krumm EA, Patel VJ, Tillery TS, Yasrebi A, Shen J, Guo GL, et al. Organophosphate Flame-Retardants Alter Adult Mouse Homeostasis and Gene Expression in a Sex-Dependent Manner Potentially Through Interactions With ERα. Toxicol Sci. 2018;162(1):212–24. [PubMed: 29112739]
100. Adams S, Wiersielis K, Yasrebi A, Conde K, Armstrong L, Guo GL, et al. Sex- and age-dependent effects of maternal organophosphate flame-retardant exposure on neonatal hypothalamic and hepatic gene expression. Reprod Toxicol. 2020;94:65–74. [PubMed: 32360330]
101. Belcher SM, Cookman CJ, Patisaul HB, Stapleton HM. In vitro assessment of human nuclear hormone receptor activity and cytotoxicity of the flame retardant mixture FM 550 and its triarylphosphate and brominated components. Toxicol Lett. 2014.
102. Liu X, Ji K, Choi K. Endocrine disruption potentials of organophosphate flame retardants and related mechanisms in H295R and MVLN cell lines and in zebrafish. Aquat Toxicol. 2012;114-115:173–81. [PubMed: 22446829]
103. McCarthy MM, Auger AP, Bale TL, De Vries GJ, Dunn GA, Forger NG, et al. The epigenetics of sex differences in the brain. J Neurosci. 2009;29(41):12815–23. [PubMed: 19828794]
104. Abel JL, Rissman EF. Location, location, location: genetic regulation of neural sex differences. Rev Endocr Metab Disord. 2012;13(3):151–61. [PubMed: 21607612]
105. Acaz-Fonseca E, Ortiz-Rodriguez A, Garcia-Segura LM, Astiz M. Sex differences and gonadal hormone regulation of brain cardiolipin, a key mitochondrial phospholipid. J Neuroendocrinol. 2020;32(1):e12774. [PubMed: 31323169]
106. Cao J, Patisaul HB. Sexually dimorphic expression of hypothalamic estrogen receptors alpha and beta and kiss1 in neonatal male and female rats. J Comp Neurol. 2011;519(15):2954–77. [PubMed: 21484804]
107. Cao J, Patisaul HB. Sex specific expression of estrogen receptors alpha and beta and kiss1 in the postnatal rat amygdala. J Comp Neurol. 2013;521(2):465–78. [PubMed: 22791648]
108. Acaz-Fonseca E, Ortiz-Rodriguez A, Lopez-Rodriguez AB, Garcia-Segura LM, Astiz M. Developmental Sex Differences in the Metabolism of Cardiolipin in Mouse Cerebral Cortex Mitochondria. Sci Rep. 2017;7:43878. [PubMed: 28262723]
109. Santoro A, Mele E, Marino M, Viggiano A, Nori SL, Meccariello R. The Complex Interplay between Endocannabinoid System and the Estrogen System in Central Nervous System and Periphery. Int J Mol Sci. 2021;22(2).
110. Ventura-Clapier R, Moulin M, Piquereau J, Lemaire C, Mericskay M, Veksler V, et al. Mitochondria: a central target for sex differences in pathologies. Clin Sci (Lond). 2017;131(9):803–22. [PubMed: 28424375]
111. Klinge CM. Estrogenic control of mitochondrial function. Redox Biol. 2020;31:101435. [PubMed: 32001259]
112. Werling DM, Geschwind DH. Sex differences in autism spectrum disorders. Curr Opin Neurol. 2013;26(2):146–53. [PubMed: 23406909]
113. McCarthy MM, Wright CL. Convergence of Sex Differences and the Neuroimmune System in Autism Spectrum Disorder. Biol Psychiatry. 2017;81(5):402–10. [PubMed: 27871670]
114. May T, Adesina I, McGillivray J, Rinehart NJ. Sex differences in neurodevelopmental disorders. Curr Opin Neurol. 2019;32(4):622–6. [PubMed: 31135460]

115. Nguon K, Ladd B, Baxter MG, Sajdel-Sulkowska EM. Sexual dimorphism in cerebellar structure, function, and response to environmental perturbations. Prog Brain Res. 2005;148:341–51. [PubMed: 15661202]

116. Rebuli ME, Patisaul HB. Assessment of sex specific endocrine disrupting effects in the prenatal and pre-pubertal rodent brain. The Journal of steroid biochemistry and molecular biology. 2016;160:148–59. [PubMed: 26307491]

117. Frye RE, Cakir J, Rose S, Palmer RF, Austin C, Curtin P, et al. Mitochondria May Mediate Prenatal Environmental Influences in Autism Spectrum Disorder. J Pers Med. 2021;11(3).

118. Wong S, Giulivi C. Autism, Mitochondria and Polybrominated Diphenyl Ether Exposure. CNS Neurol Disord Drug Targets. 2016;15(5):614–23. [PubMed: 27071785]

119. Davies KL, Smith DJ, El-Bacha T, Stewart ME, Easwaran A, Wooding PFP, et al. Development of cerebral mitochondrial respiratory function is impaired by thyroid hormone deficiency before birth in a region-specific manner. FASEB J. 2021;35(5):e21591. [PubMed: 33891344]

120. Prezioso G, Giannini C, Chiarelli F. Effect of Thyroid Hormones on Neurons and Neurodevelopment. Horm Res Paediatr. 2018;90(2):73–81. [PubMed: 30157487]

121. Goodchild C, Karouna-Renier NK, Henry PFP, Letcher RJ, Schultz SL, Maddox CM, et al. Thyroid disruption and oxidative stress in American kestrels following embryonic exposure to the alternative flame retardants, EHTBB and TBPH. Environ Int. 2021;157:106826. [PubMed: 34438233]

122. Springer C, Dere E, Hall SJ, McDonnell EV, Roberts SC, Butt CM, et al. Rodent thyroid, liver, and fetal testis toxicity of the monoester metabolite of bis-(2-ethylhexyl) tetrabromophthalate (tbph), a novel brominated flame retardant present in indoor dust. Environ Health Perspect. 2012;120(12):1711–9. [PubMed: 23014847]

123. Santos MS, Li H, Voglmaier SM. Synaptic vesicle protein trafficking at the glutamate synapse. Neuroscience. 2009;158(1):189–203. [PubMed: 18472224]

124. Augustin SM, Lovinger DM. Functional Relevance of Endocannabinoid-Dependent Synaptic Plasticity in the Central Nervous System. ACS Chem Neurosci. 2018;9(9):2146–61. [PubMed: 29400439]

125. Bruel-Jungerman E, Lucassen PJ, Francis F. Cholinergic influences on cortical development and adult neurogenesis. Behav Brain Res. 2011;221(2):379–88. [PubMed: 21272598]

126. Vos M, Lauwers E, Verstreken P. Synaptic mitochondria in synaptic transmission and organization of vesicle pools in health and disease. Front Synaptic Neurosci. 2010;2:139-. [PubMed: 21423525]

127. Mattson MP, Gleichmann M, Cheng A. Mitochondria in neuroplasticity and neurological disorders. Neuron. 2008;60(5):748–66. [PubMed: 19081372]

128. Yuan L, Li J, Zha J, Wang Z. Targeting neurotrophic factors and their receptors, but not cholinesterase or neurotransmitter, in the neurotoxicity of TDCPP in Chinese rare minnow adults (Gobiocypris rarus). Environmental Pollution. 2016;208:670–7. [PubMed: 26552522]

129. Shi Q, Wang M, Shi F, Yang L, Guo Y, Feng C, et al. Developmental neurotoxicity of triphenyl phosphate in zebrafish larvae. Aquatic Toxicology. 2018;203:80–7. [PubMed: 30096480]

130. Shi Q, Guo W, Shen Q, Han J, Lei L, Chen L, et al. In vitro biolayer interferometry analysis of acetylcholinesterase as a potential target of aryl-organophosphorus flame-retardants. Journal of Hazardous Materials. 2021;409:124999. [PubMed: 33454525]

131. Dasgupta S, Ray SK. Diverse Biological Functions of Sphingolipids in the CNS: Ceramide and Sphingosine Regulate Myelination in Developing Brain but Stimulate Demyelination during Pathogenesis of Multiple Sclerosis. J Neurol Psychol. 2017;5(1).

132. Mencarelli C, Martinez-Martinez P. Ceramide function in the brain: when a slight tilt is enough. Cell Mol Life Sci. 2013;70(2):181–203. [PubMed: 22729185]

133. Cruciani-Guglielmacci C, López M, Campana M, le Stunff H. Brain Ceramide Metabolism in the Control of Energy Balance. Frontiers in Physiology. 2017;8.

134. Kolesnick RN, Krönke M. Regulation of ceramide production and apoptosis. Annu Rev Physiol. 1998;60:643–65. [PubMed: 9558480]

135. Bernhard W, Poets CF, Franz AR. Choline and choline-related nutrients in regular and preterm infant growth. European Journal of Nutrition. 2019;58(3):931–45. [PubMed: 30298207]

136. Dergunov AD, Rosseneu M. The significance of apolipoprotein E structure to the metabolism of plasma triglyceride-rich lipoproteins. Biol Chem Hoppe Seyler. 1994;375(8):485–95. [PubMed: 7811390]

137. Mahley RW, Weisgraber KH, Huang Y. Apolipoprotein E: structure determines function, from atherosclerosis to Alzheimer's disease to AIDS. J Lipid Res. 2009;50 Suppl(Suppl):S183–8. [PubMed: 19106071]

138. Serrano-Pozo A, Das S, Hyman BT. APOE and Alzheimer's disease: advances in genetics, pathophysiology, and therapeutic approaches. Lancet Neurol. 2021;20(1):68–80. [PubMed: 33340485]

139. Wójtowicz S, Strosznajder AK, Jeżyna M, Strosznajder JB. The Novel Role of PPAR Alpha in the Brain: Promising Target in Therapy of Alzheimer's Disease and Other Neurodegenerative Disorders. Neurochem Res. 2020;45(5):972–88. [PubMed: 32170673]

140. Wada Y, Maekawa M, Ohnishi T, Balan S, Matsuoka S, Iwamoto K, et al. Peroxisome proliferator-activated receptor α as a novel therapeutic target for schizophrenia. EBioMedicine. 2020;62:103130. [PubMed: 33279456]

141. Tung EWY, Ahmed S, Peshdary V, Atlas E. Firemaster® 550 and its components isopropylated triphenyl phosphate and triphenyl phosphate enhance adipogenesis and transcriptional activity of peroxisome proliferator activated receptor (Pparγ) on the adipocyte protein 2 (aP2) promoter. PLoS One. 2017;12(4):e0175855. [PubMed: 28437481]

142. Bond KM, McCarthy MM, Rubin JB, Swanson KR. Molecular omics resources should require sex annotation: a call for action. Nat Methods. 2021;18(6):585–8. [PubMed: 34099934]

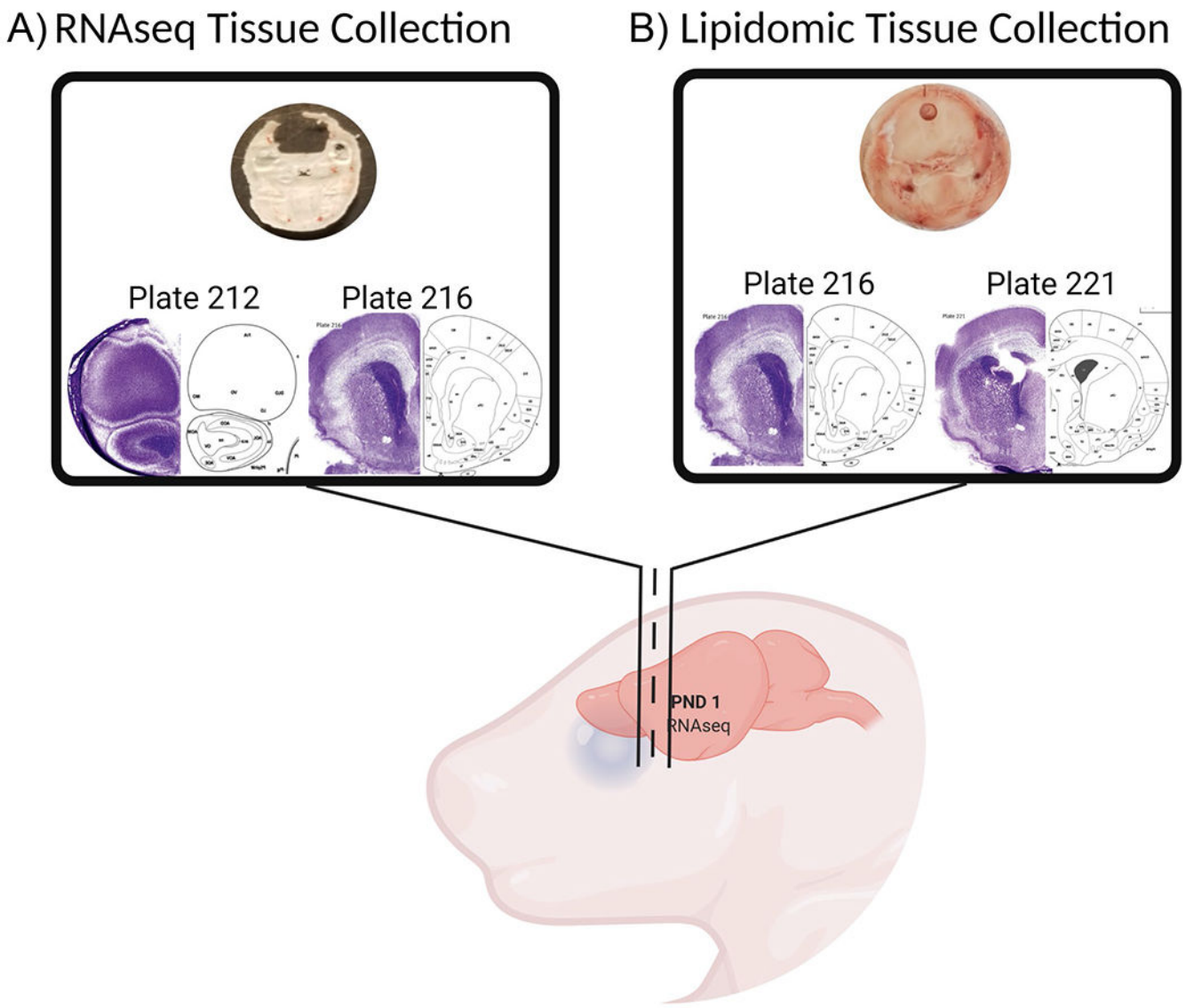

Figure 1.

Illustration of how cortical tissue for RNAseq and lipidomic analysis was collected in the PND1 offspring gestationally exposed to FM 550, BFR or OPFR. A) For RNAseq analysis, whole PND1 heads were cryosectioned at 20 μm and the forebrain slices collected using The Developing Rat Nervous System (Paxinos and Ashwell 2018) atlas as a guide. Tissue collection began on plate 212 as indicated by clear separation of cortex and olfactory bulb and stopped on plate 216, recognized by the distinct position of the corpus collosum, fornix and lateral ventricle. B) For lipidomic tissue collection, micropunches (1.25mm width by 1-1.15 mm deep) were then used to isolate the medial portion of the cortex from the same PND1 mounted heads. The isolated lipidomics tissue approximately contained cortical material from plates 216 – 221.

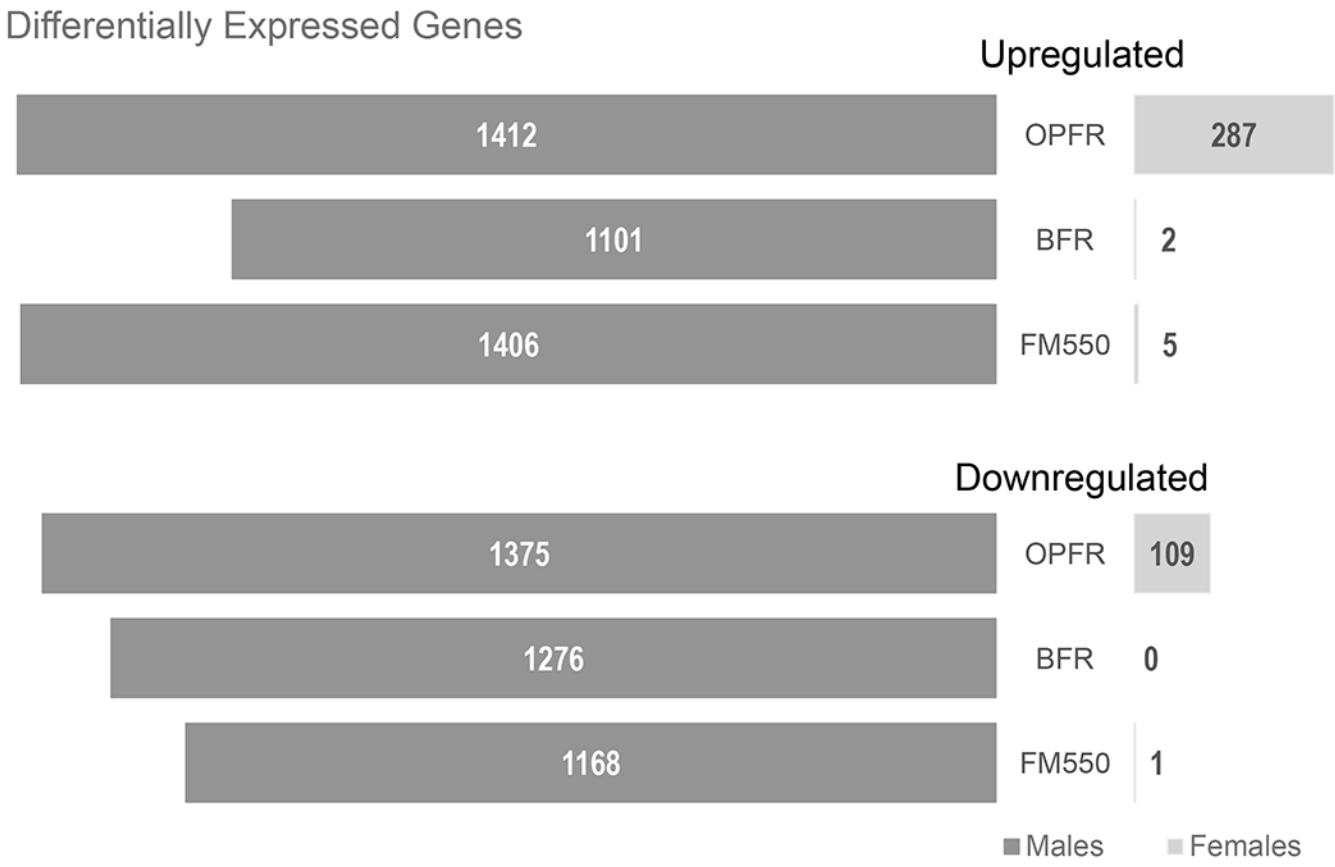

Figure 2.

Differentially expressed genes (DEGs) separated by sex, exposure group and direction of expression change. Males had the highest number of DEGs regardless of exposure group, with only OPFR females having greater than 100 DEGs in both directions. For this reason, data from all the male exposure groups, but only the OPFR female exposure group, underwent pathways analysis.

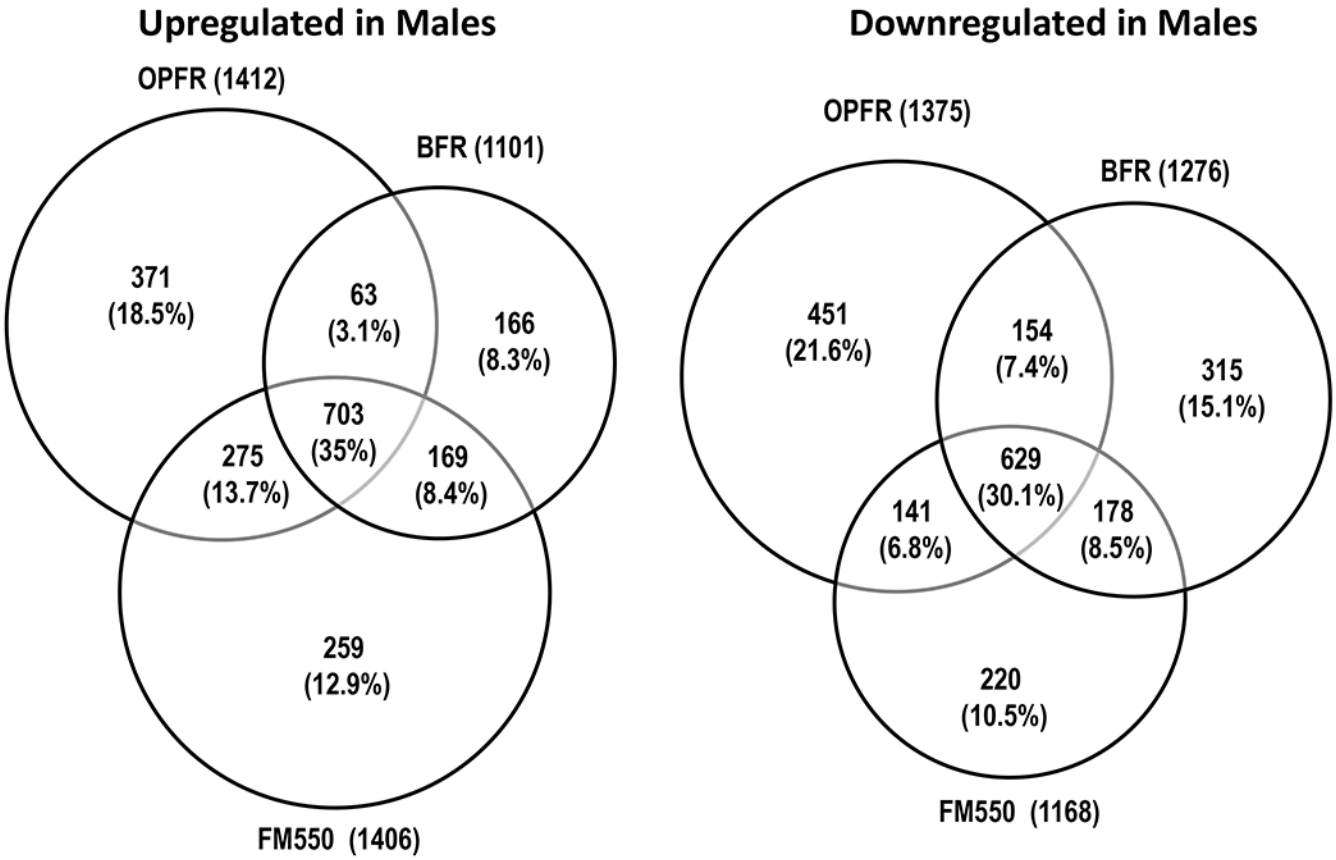

Figure 3.

Shared DEGs by direction across exposure group in males. Across all three exposure groups, 35% of upregulated (703) and 30.1% of downregulated (629) genes were identified as shared DEGs. The FM550 and BFR groups had 8.4% upregulated and 8.5% downregulated genes in common, while the FM550 and OPFR groups had 13.7% upregulated and 6.8% downregulated genes in common.

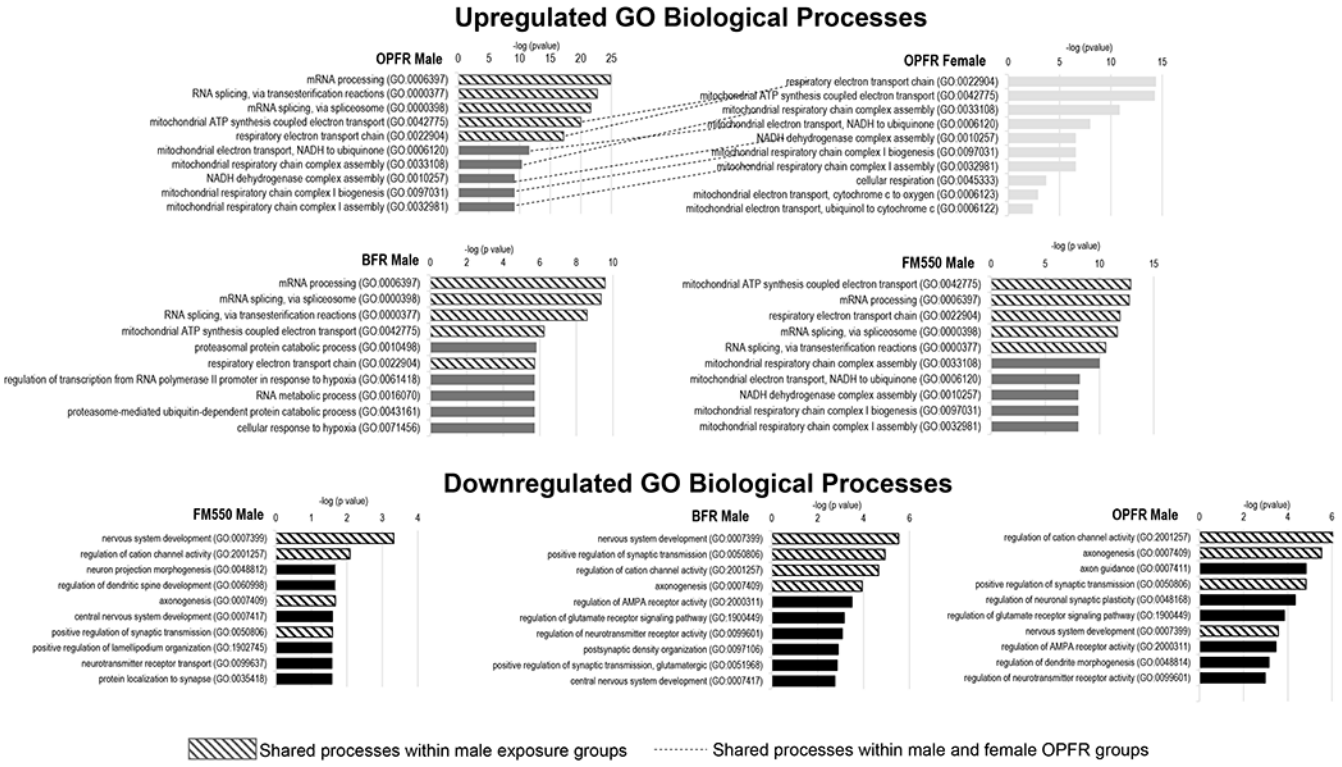

Figure 4.

Summary of the ten most significant upregulated and downregulated GO Biological Processes in the exposure groups examined. Five upregulated processes were shared across all groups (hatched bars). Within the OPFR male and females 6 upregulated processes were shared by both sexes (connected with dashed lines). Four downregulated process were shared across all groups examined (hatched bars). OPFR females had no downregulated processes.

A) List of the 22 Upregulated KEGG Pathways Shared by all Male Exposure Groups:

- Parkinson disease*
- Huntington disease*
- Oxidative phosphorylation*
- Alzheimer disease*
- Pathways of neurodegeneration*
- Prion disease
- Amyotrophic lateral sclerosis
- Thermogenesis
- Diabetic cardiomyopathy
- Non-alcoholic fatty liver disease
- Spliceosome
- RNA transport
- Proteasome
- Spinocerebellar ataxia
- RNA degradation
- Protein export
- Protein processing in endoplasmic reticulum
- Basal transcription factors
- RNA polymerase
- mRNA surveillance pathway
- Ubiquitin mediated proteolysis
- Cell cycle

B) List of the 12 Upregulated KEGG Pathways Shared by OPFR Males and Females:

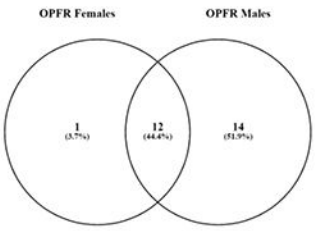

Oxidative phosphorylation*
Parkinson disease*
Thermogenesis
Prion disease
Huntington disease*
Diabetic cardiomyopathy
Amyotrophic lateral sclerosis
Non-alcoholic fatty liver disease
Pathways of neurodegeneration*
Alzheimer disease*
Retrograde endocannabinoid signaling
Cardiac muscle contraction

C) Genes Shared Across the Neurodegenerative Disease Pathways Enriched in Both Sexes:

ATP5F1E	COX7A2	NDUFB11
ATP5ME	COX7C	NDUFB4
ATP5PD	ND3	SEM1
ATP5PF	NDUFA12	TUBB2A
COX17	NDUFA2	UQCRB
COX6B1	NDUFA3	UQCRH

Figure 5.

Upregulated KEGG pathways. A) List of 22 upregulated KEGG pathways shared by OPFR, BFR and FM550 males. B) List of the 12 upregulated KEGG pathways shared between the OPFR males and females. The five neuronal degenerative pathways both sexes had in common are indicated by *. C) List of the 18 genes shared across the 5 neuronal degenerative pathways enriched in the OPFR exposed groups. All are involved in cellular respiration.

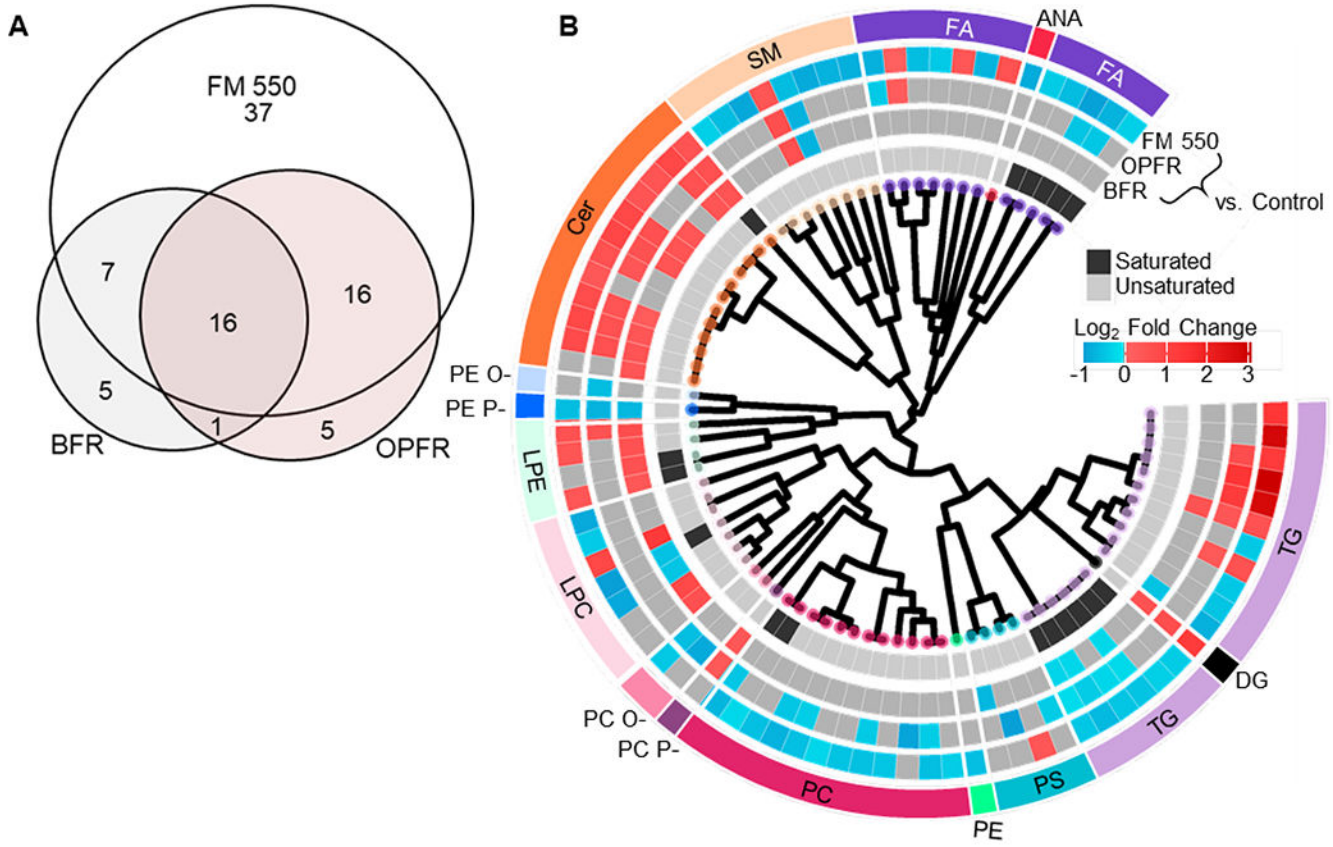

Figure 6.

Statistically significant lipids observed in all exposure versus control comparaisons. **A)** Venn diagram of statistically significant lipids from each exposure comparison and their overlap. **B)** Circular dendrogram of all 87 statistically significant lipids generated with an ECFP6 fingerprint, Tanimoto distance, and average linkage for the corresponding exposure comparisons. Log_2 fold change is overlaid for all three comparisons to visualize trends in significant dysregulation. All identified lipids without statistically significance are shown in grey whereas statistically significant species that were either upregulated or downregulated are displayed in red and blue. Lipid class abbreviations include: FA = fatty acid, ANA = anandamide, SM = sphingomyelin, Cer = ceramide, PE O- = ether-linked phosphatidylethanolamine, PE P- = vinyl ether-linked phosphatidylethanolamine, LPE = lysophosphatidylethanolamine, LPC = lysophosphatidylcholine, PC O- = ether-linked phosphatidylcholine, PC P- = vinyl ether-linked phosphatidylcholine, PC = phosphatidylcholine, PE = phosphatidylethanolamine, PS = phosphatidylserine, TG = triglyceride, DG = diglyceride.

Group	Sex	Upregulated	Downregulated	Total
Control	Male	-	-	
Control	Female	-	-	
BFR	Male	4	8	12
BFR	Female	9	3	12
OPFR	Male	2	18	20
OPFR	Female	15	6	21
FM 550	Male	16	35	51
FM 550	Female	18	25	43

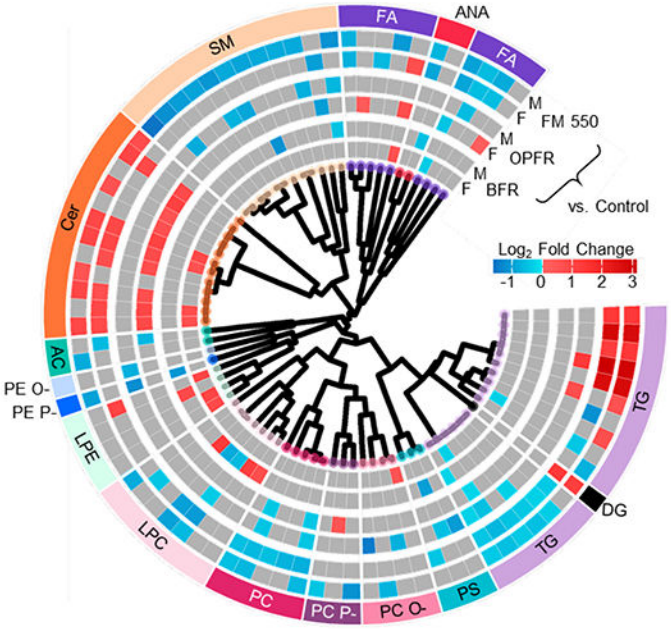

Figure 7.

Sex specific statistically significant lipids observed in exposure versus control comparisons. Circular dendrogram illustrating Female only (F) and Male only (M) comparisons. Log_2 fold change is overlaid for all six comparisons to visualize trends in significant dysregulation. All identified but insignificant lipids are shown in grey whereas statistically significant species that were either upregulated or downregulated are displayed in red and blue. Lipid class abbreviations include: FA = fatty acid, ANA = anandamide, SM = sphingomyelin, Cer = ceramide, AC = acylcarnitine, PE O- = ether-linked phosphatidylethanolamine, PE P- = vinyl ether-linked phosphatidylethanolamine, LPE = lysophosphatidylethanolamine, LPC = lysophosphatidylcholine, PC = phosphatidylcholine, PC O- = ether-linked phosphatidylcholine, PC P- = vinyl ether-linked phosphatidylcholine, PS = phosphatidylserine, TG = triglyceride, DG = diglyceride

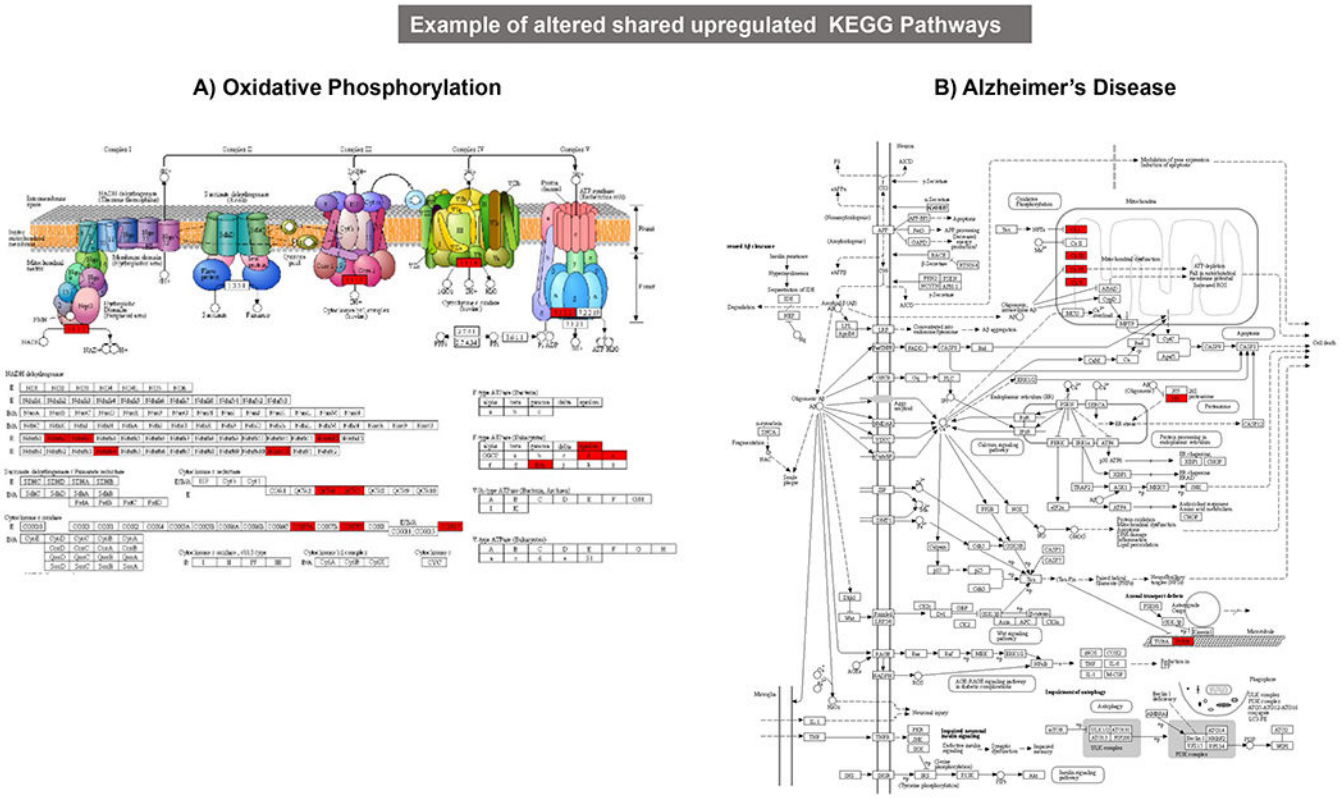

Figure 8.

Example of how enriched genes factor into the identified upregulated KEGG pathways. The 18 commonly expressed genes within the neurodegenerative disease pathways identified were used to render KEGG pathways using Pathview (http://bioinformatics.sdstate.edu/go/). Depicted in red are FR-affected genes in the oxidative phosphorylation (A) and Alzheimer's disease (B) pathways.

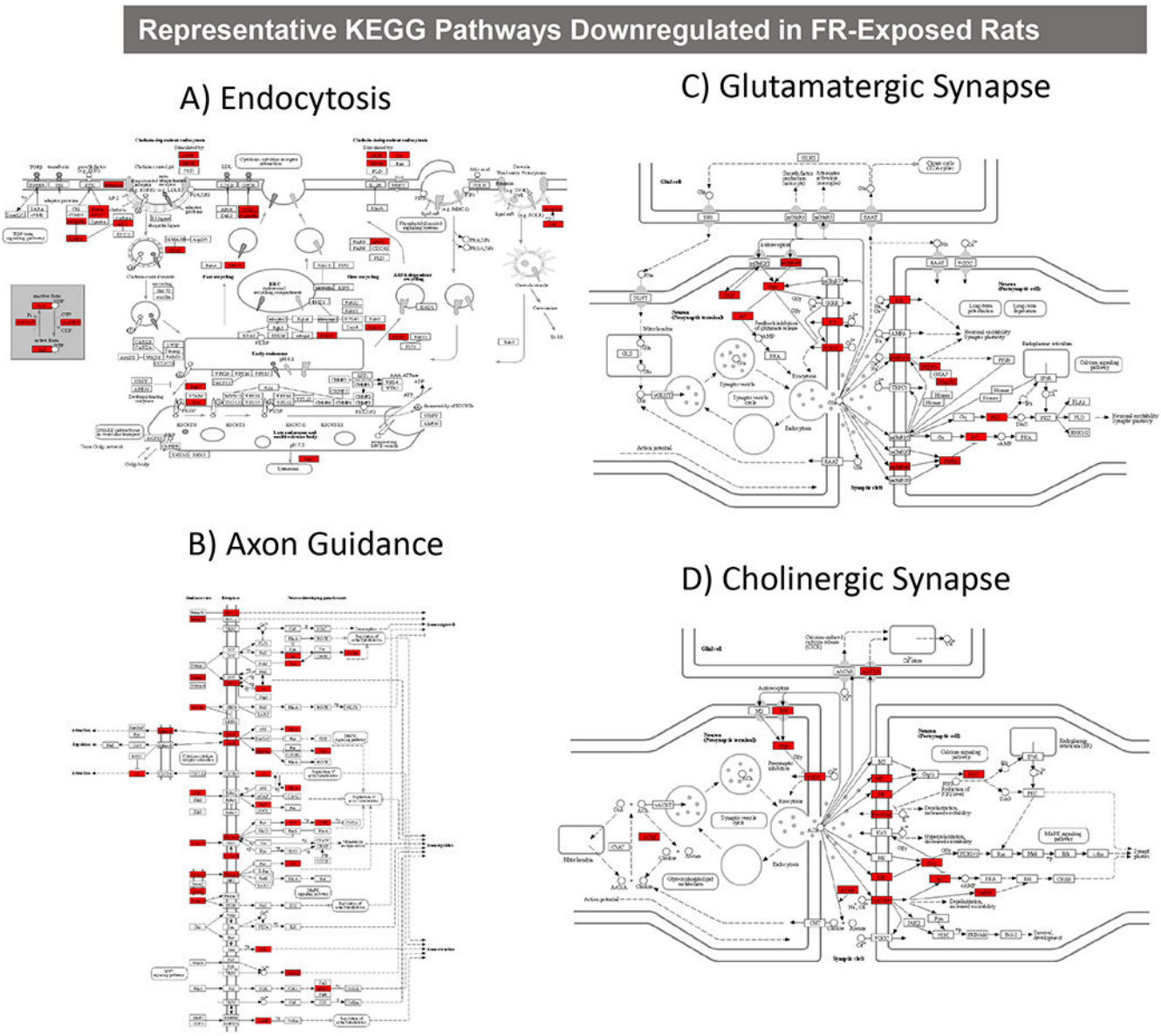

Figure 9.

Representative renderings of 4 downregulated KEGG pathways in the exposed groups. DEGs within each are depicted in red. A) Endocytosis was the only downregulated pathway shared across all male exposure groups and the OPFR females. B) Axon guidance was the only significant downregulated pathway in both OPFR males and females. C & D) In males, OPFR downregulated KEGG pathways included glutamatergic and cholinergic synapses.

Table 1.

Predicted Transcription Factor Protein-Protein Interaction (PPI)

	OPFR	BFR	FM550	Shared
Upregulated	ILF3, ESR1, POLR2A, TARDBP, BRCA1, MYC, NANOG, RAD21, CHD1, ILF2, RNF2, CTCF, SMC3, FOXP3, ELF1, HTT, TBP, TAF1, TRIM28, HDAC2, BRF2, TP63, POU5F1, TP53, NR3C1, SUZ12, UPF1, HSF1, VDR, TAF7, PML, ESRRA, AHR, IKZF1, POLE, ETS1, ESRRB, IRF1, IRF3, REST, HCFC1, SP3	ESR1, ILF3, POU5F1, MYC ILF2, TRIM28, UPF1, NANOG, CTNNB1, BRCA1, TARDBP, TBP, RAD21, ATF2, FOXP3, NFKB1 CTCF, HTT, SIRT3, POLR2A, KDM5A, PML, HSF1, UBTF, ERG, TP53, TAF1, EED, AIRE, RNF2, TP63	ESR1, ILF3, UPF1, TARDBP, BRCA1, CTNNB1, TRIM28, MYC, TBP, RAD21, ATF2, ILF2, HDAC2, PML, POU5F1, TP53, CTCF, POLR2A, HSF1, SMC3, NANOG, HTT, FOS, SMAD2	ESR1, HTT, POU5F1, ILF3, ILF2, POLR2A, TARDBP, BRCA1, MYC, NANOG, RAD21, CTCF, TBP, TRIM28, TP53, UPF1, HSF1, PML
Downregulated		RXRA, EP300, STAT5A	RXRA	RXRA

Hub proteins predicted to be up or downregulated in the males of each group. In total there were 18 commonly upregulated and 1 downregulated PPIs predicted. No predicted PPIs were identified for the OPFR females.